Geoderma 432 (2023) 116414

Contents lists available at ScienceDirect

Geoderma

journal homepage: www.elsevier.com/locate/geoderma

# Functional variability in specific root respiration translates to autotrophic differences in soil respiration in a temperate deciduous forest

J. Aaron Hogan [a,e,*], Jessy L. Labbé [b,f], Alyssa A. Carrell [b], Jennifer Franklin [c], Kevin P. Hoyt [d], Oscar J. Valverde-Barrantes [a], Christopher Baraloto [a], Jeffrey M. Warren [e]

[a] Institute of Environment, Department of Biological Sciences, Florida International University, Miami, FL 33199, USA
[b] Biosciences Division, Oak Ridge National Laboratory, Oak Ridge, TN 37830, USA
[c] Department of Forestry, Wildlife & Fisheries, University of Tennessee, Knoxville, TN 37996, USA
[d] University of Tennessee Forest Resources AgResearch and Education Center, Oak Ridge, TN 37830, USA
[e] Environmental Sciences Division and Climate Change Science Institute, Oak Ridge National Laboratory, Oak Ridge, TN 37830, USA
[f] Invaio Sciences, Cambridge, MA 02138, USA

ARTICLE INFO

Handling Editor: Jan Willem Van Groenigen

*Keywords:*
Belowground physiology
Root functional traits
Soil fungi and bacteria
Soil microbial nitrogen
ZeroTol
Temperate forest

ABSTRACT

$CO_2$ release from forest soils ($R_s$) is a prominent flux in the global carbon cycle. $R_s$ is derived from roots (autotrophic respiration, $R_a$) and microbial (heterotrophic) respiration and is highly dynamic, as it depends on edaphic and environmental conditions as well as root functional traits and microbial community composition. It is unclear how root functional traits affect root and microbial respiration rates; however, their consideration may help parse out the relative contributions of root and microbial respiration to $R_s$. At a temperate forest site, root systems of 3–4 functional root orders and their surrounding surface soil were carefully excavated and placed into custom trays designed to repeatedly measure $R_s$ *in situ* on eight temperate tree species that varied in their root functional strategies and mycorrhizal affinity. $R_s$ was measured bi-weekly to monthly for nearly one year using a custom chamber attached to a gas exchange system. $R_s$ varied over time, ranging from 0.3 to 12 μmol $m^{-2}$ $s^{-1}$. Comparable root systems of the same species were *excised* from the soil and specific root respiration rates ($R_r$) were measured. $R_r$ ranged from 2.5 to 9.0 nmol $g^{-1}$ $s^{-1}$ and was negatively correlated with root tissue density and positively related to root tissue nitrogen concentration. Using $R_r$ to estimate $R_a$, we estimate that $R_a$ accounts for <10%, on average 2–3%, of $R_s$ for individual root systems (averaging 1.2 g dry biomass) housed in surrounding soil (average 1.3 kg dry mass) *in situ*; thus, $R_a$ was roughly 20 times greater than $R_h$ per unit mass. The contribution of $R_a$ peaked in the fall and coincided with leaf senescence of the forest canopy. A soil-sterilizing experimental treatment designed to help isolate $R_a$ *in situ* reduced bacterial biomass and shifted fungal community composition, but there was no reduction in $R_s$ of the *in-situ* root-soil tray systems. The relative $R_a$ to $R_s$ ratio increased with root functional strategies characterized by greater specific root length and tip abundance, but also to greater root tissue density. The ratio of $R_a$ to $R_s$ also increased with warmer soil temperatures and decreased slightly with increasing soil moisture. We discuss how incorporating root functional traits as modulators of the autotrophic contribution to $R_s$ could be considered when modeling total soil $CO_2$ efflux from forests.

*Abbreviations:* $CO_2$, carbon dioxide; $R_s$, belowground respiration (including autotrophic and heterotrophic components); C, carbon; $R_r$, root tissue specific respiration rate (mass-based); $R_a$, autotrophic (*i.e.*, root-derived) belowground respiration; $N_{root}$, root nitrogen concentration; RTD, root tissue density; AM, arbuscular mycorrhizal; ECM, ectomycorrhizal; $R_a/R_s$, the contribution of root (*i.e.*, autotrophic) respiration to soil respiration; SLA, specific leaf area; $C_{root}$, root carbon concentration; $C_{leaf}$, leaf carbon concentration; $N_{leaf}$, leaf nitrogen concentration; $P_{leaf}$, leaf phosphorus concentration; SRL, specific root length; SRA, specific root area; N, nitrogen; TC, soil total organic carbon; DOC, soil dissolved organic carbon; MBC, microbial biomass carbon; TN, soil total nitrogen; DN, soil dissolved nitrogen; MBN, microbial biomass nitrogen; ANOVA, analysis of variance; HSD, Tukey's post-hoc test for honest significant differences; PCA, principal components analysis; SRTA, specific root tip abundance.

* Corresponding author at: University of Florida, Dept. of Biology, P.O. Box 118525, 220 Bartram Hall, Gainesville, FL 32611-8525, USA.
*E-mail address:* hogan.jaaron@ufl.edu (J. Aaron Hogan).

https://doi.org/10.1016/j.geoderma.2023.116414
Received 4 July 2022; Received in revised form 30 January 2023; Accepted 27 February 2023

## 1. Introduction

Soil carbon dioxide ($CO_2$) efflux, or belowground respiration ($R_s$), is a dominant process in the carbon (C) cycling of forests (Janssens et al., 2001; Raich and Nadelhoffer, 1989; Xu and Shang, 2016). Globally, $R_s$ represents the second-largest flux in the global C cycle behind only gross primary production (~130 pG C per year, Madani et al., 2020), accounting for 85–110 pG C per year (Bond-Lamberty and Thomson, 2010a; b; Raich et al., 2002). $R_s$ is strongly influenced by soil temperature and moisture, but these are inherently linked to both climate and vegetation types (*e.g.*, coniferous vs. broadleaf evergreen forests). For example, climate accounted for nearly half of the variation in $R_s$ in three coniferous forest types in Oregon with stand age and disturbance history also being significant sources of variation (Campbell and Law, 2005). Comparisons of $R_s$ within forests located in the same climatic zone have reported $R_s$ rates in broadleaf forests to be greater than those in coniferous forests (Raich and Tufekciogul, 2000; Wang et al., 2006). Differences in $R_s$ between forest types and under different tree species may arise because of species influences on the soil environment (*e.g.*, temperature, moisture), variation in litter quantity and chemistry, differences in root density and distribution, variation in root structure and function, and interactions between plant roots and microbial communities.

$R_s$ has distinct autotrophic and heterotrophic components (Hanson et al., 2000; Kuzyakov, 2006; Ryan and Law, 2005). The heterotrophic component ($R_h$) arises primarily from microbial respiration in the soil, mycorrhizal hyphae, and soil fauna, whereas the autotrophic component ($R_a$) mainly comes from plant root respiration. Although species differ in their specific root (*i.e.*, mass-based tissue) respiration rates ($R_r$, Burton et al. 2002; Makita et al. 2012; Roumet et al., 2016), variation in fine root biomass in the upper soil is the principal driver of variation in $R_s$ in forest ecosystems (Pregitzer et al., 2008; Wang et al., 2017). Spatial variation in the amount and metabolic activity of root tissues makes the contribution of root-derived autotrophic respiration ($R_a$) to $R_s$ highly variable. Across forest ecosystems, $R_a$ comprises roughly 42-46% of $R_s$, but is normally distributed across a broad range from <10% to >90% (Hanson et al., 2000; Jian et al., 2022). The large range in estimates arises from the multitude of methods used for measuring $R_s$ and quantifying $R_a$ (Bond-Lamberty et al., 2011; Hanson et al., 2000; Ryan and Law, 2005), as well as species differences, and soil edaphic and stand characteristics.

Plants have wide-ranging water and resource-use strategies that regulate plant life history characteristics (*e.g.*, growth, photosynthesis, and plant tissue respiration rates) (Craine and Dybzinski, 2013, Reich, 2014). Functional traits are good indicators of variation in plant strategy (Adler et al., 2014; Díaz et al., 2016), with more acquisitive species with fast life histories typically having greater specific leaf area (SLA) and specific root length (SRL) and lower wood densities. The degree to which species variation in resource-use strategies translates to effects on $R_s$ is not well understood. Species differences can affect $R_s$ through varying magnitudes in $R_a$ or variation in soil resource extraction, root production, turnover, and biomass (Roumet et al 2016). Alternatively, species might differentially affect the magnitude of $R_s$ via $R_h$ due to variation in exudate production or litter input quality (*i.e.*, recalcitrance, N content) that influence the size, composition, and activity of the soil microbiome. Thus, soil respiration is intertwined with plant root C dynamics, which is not often considered empirically in models of $R_s$ (*e.g.*, Blagodatsky and Smith, 2012; Fang and Moncrieff, 1999). This indicates a pressing need to improve estimates of root contributions to $R_s$ (either indirectly or directly) and other C fluxes between roots and soils (Reichstein and Beer, 2008).

Root functional traits provide the potential to understand and constrain variance in $R_a$, if differences in $R_r$ can be linked to variation in $R_s$ in a meaningful way (Bergmann et al., 2020; Freschet et al., 2020; Warren et al., 2015). $R_r$ scales along the root nitrogen ($N_{root}$) - root tissue density (RTD) axis of the root functional trait space (Burton et al., 2002; Paradiso et al., 2019; Reich et al., 2008). RTD and $N_{root}$ are typically opposed in root functional trait space and represent a physiological tradeoff between tissue resource investment and lifespan (Bergmann et al., 2020; McCormack et al, 2012; McCormack and Iversen, 2019). Thus, species with faster life-history strategies typically have higher $N_{root}$ and $R_r$ (Comas et al., 2002; Makita et al., 2012), and lower root lifespans (McCormack et al, 2012) than species with slower, more-conservative life-history strategies. Additional, $R_a$ and $R_s$ are tightly interconnected via the labile carbon transfer between roots and soil microbes (Bouma et al., 1997; Cleveland et al., 2007; Hill et al., 2015; Lavigne et al., 2003; Pausch and Kuzyakov, 2018; Teodosio et al., 2017). For example, Warren et al. (2011) showed how isotopically-labeled $R_s$ was related to previous-day total sap flow in young Loblolly Pines. Thus, plant carbon dynamics (*e.g.*, photosynthesis, labile C movement to the soil, and $R_r$) are intertwined with $R_s$ through their effect on $R_h$ (*i.e.*, soil priming effects) (Högberg et al., 2001). However, it is unclear if root functional differences lead to detectable differences in $R_a$, $R_h$ or how they interact to influence $R_s$.

An additional and orthogonal axis of root functional variation to the RTD-$N_{root}$ tradeoff is the degree of mycorrhizal association, commonly represented by mycorrhizal type (*i.e.*, arbuscular mycorrhizal: AM vs. ectomycorrhizal: ECM association) (Bergmann et al., 2020; McCormack and Iversen, 2019; Yan et al., 2022). RTD variation among AM and ECM tree species has been hypothesized to reflect evolved anatomical facilitation of fungal hyphae growth into roots, with AM taxa generally having greater root cortex-to-stele ratios and lower tissue densities than ECM taxa (Comas et al., 2014; McCormack and Iversen, 2019; Yan et al., 2022). Association with ECM or AM species can create differences in ecosystem-level functioning, including modulating tree species competitive strength, recruitment dynamics, stand biomass and soil inputs (Bennett et al., 2017; Johnson et al., 2018; Soudzilovskaia et al., 2019). Several studies have shown that $R_s$ is greater under AM trees than ECM trees (Lang et al., 2020; Taylor et al., 2016; Wurzburger and Brookshire, 2017). At least some of this increase in $R_s$ for AM trees relative to ECM trees is related to the respiratory cost of mycorrhizal association, which is estimated at 2–17%, via an increase in $R_h$ (Bryla and Eissenstat, 2005). Additionally, AM trees tend to produce more labile root tissue litter, which exerts distinct effects on soil C pools, contributing up to twice as much root-derived C to soils as ECM species (Keller et al., 2021), and doubling rates of soil C decomposition and cycling potentially via increased soil microbial enzyme activity (Liming et al., 2021). Thus, it is not unreasonable to expect that differences in $R_a$, because variation in $R_r$ and different root functional strategies between AM and ECM species, contribute to variation in $R_s$.

Moreover, variation in $R_s$ due to the influence of tree species or mycorrhizal type on soil microbiomes and their dynamics over time and in response to environmental conditions is not entirely understood, especially at the physiological scale of functional root systems (*i.e.*, entire root units containing 3–4 orders of the most-physiologically active fine roots). In this paper, we present a novel methodology to measure $R_s$ of entire fine root system segments and their surrounding soil *in situ*, and we employ the method to understand the linkage of $R_a$ to $R_s$. Using eight tree species from a North American deciduous forest, we asked:

- *How do rates of root respiration relate to interspecific differences in root functional strategy?* Since thicker root diameters indicate a conservative functional strategy (Bergmann et al., 2020; Eissenstat et al., 2015), we expected species with thinner roots to have higher specific root respiration rates than species with thicker roots. Tree species with thick roots (*e.g.*, basal Angiosperms) are usually AM hosts (Valverde-Barrantes et al., 2017), which may have different root functional trait – $R_r$ relationships than ECM species (Burton et al., 2002; Gao et al., 2021).
- *Does the contribution of autotrophic (i.e., root) respiration to total belowground $CO_2$ efflux ($R_a/R_s$) vary with species and root functional*

*strategy (including mycorrhizal association type)?* We hypothesized that $R_r$ might lead to a difference in $R_a/R_s$ and that species with higher measured $R_r$ should have greater $R_a/R_s$. Concerning mycorrhizal type, we expected that ECM species should have more significant heterotrophic components (*Rh*) of $R_s$ than AM species, thus decreasing $R_a/R_s$, when $R_r$ is equal.

- *Does manipulating the soil microbiome (i.e., fungal, and bacterial abundance and composition) affect $R_a/R_s$?* $R_a$ can interact with $R_h$ in complex ways to influence $R_s$, so we used an experimental manipulation aimed at reducing $R_h$, via soil sterilization. We expected $R_a$ to contribute more to $R_s$ where the experimental treatment was applied.

## 2. Methods

### 2.1. Study site

The study was carried out at the University of Tennessee Forest Resources AgResearch and Education Center in Oak Ridge, Tennessee (35.9935°N, 84.2201°W). The study area was located on the Chestnut Ridge research area to the northwest of the Arboretum grounds (Fig. S1). The site's soils are classified as Fullerton cherty silt loam (Typic Paleudult, clayey, kaolinitic, and thermic) with a bulk density of about 1.3 g $cm^{-3}$. These soils have a moderately fine granular texture, comprise about 15% gravel, and are hence, well-drained. They are dark greyish brown, mottled with yellowish-red, moderately acidic, and highly fertile (Luxmoore, 1982). From June 2019 to August 2020 (*i.e.*, during the period of this study), cumulative monthly precipitation averaged 145 ± 13.1 (standard error) mm, and average maximum and minimum daily temperatures were 21.2 ± 0.3 °C and 10.4 ± 0.3 °C, respectively (meteorological station: GHCND: USW00003841; 36.0028°N, 84.2486°W; Elevation: 275.8 m, data from Menne et al., 2012).

Forty study trees of eight species (five per species) were selected to target a range of root functional strategies (*i.e.*, sample a variety of root morphologies), as root diameter roughly scales with plant evolutionary history with older plant clades having thicker and more-variable diameter roots than more recently derived plant lineages (Valverde-Barrantes et al., 2017). The eight study species from evolutionarily oldest to youngest were: *Pinus taeda* L. (Pinaceae), *Liriodendron tulipifera* L. (Magnoliaceae), *Liquidambar styraciflua* L. (Altingiaceae), *Cercis canadensis* L. (Fabaceae), *Fagus grandifolia* L. (Fagaceae), *Acer rubrum* L. (Sapindaceae), *Nyssa sylvatica* Marshall (Nyssaceae), and *Oxydendrum arboreum* L. (DC.) (Ericaceae). Two of the eight species are ectomycorrhizal (*P. taeda, F. grandifolia,*), *O. arboreum* is ericoid mycorrhizal, while the remaining five are arbuscular mycorrhizal. *P. taeda* and *L. styraciflua* trees were found in a planted loblolly stand at the west end of the research area (see Fig. S1). *L. tulipifera* and the *C. canadensis* trees were in an area at the east of the research area, which had been clear cut with a BioBaler (Anderson Group Inc, Chesterville, Quebec, Canada) in the summer of 2011. Trees of the remaining four species were found in a mature hardwood stand between the two areas, dominated by an Eastern deciduous oak-hickory forest community (Delcourt and Delcourt, 2000). Selected trees were 5 to 20 cm in diameter at 1.3 m height, appeared healthy, and were at least 5 m apart so that root systems were less likely to overlap. Tree heights were measured using a telescoping measuring pole at the end of the experiment, and species averages ranged from 7.2 m *for C. canadensis* to 14.6 m for *N. sylvatica* and *O. arboreum*.

### 2.2. Experimental design and treatments

Eighty-six *in-situ* root system housings (hereafter trays; including six controls) were constructed (see methods S1, diagram S1, photograph S1). The *in-situ* root trays allowed for repeated measurement of soil gas flux of root systems and surrounding soil. Complete fine root systems, comprising at least three root orders (McCormack et al., 2015), were traced out from target trees and gently excavated to the first-order roots. From June 24 to June 26, 2019, two root systems per study tree were excavated and placed into the root trays in a paired design, with the transportive portion of the root system exiting a notch in the tray and still being connected to the tree. Trays were filled with soil loosened during the excavation process and recessed in the ground to be even with the soil surface. After installation, all trays were well watered and leaf litter was replaced on top. Over time, separate experimental treatments were applied to tray pairs, as described below. If a root system was damaged or broken at some point during the experiment, a new root system was established into the root tray using the same soil; this occurred for 14 of 80 root systems. Three pairs of trays not containing root systems were used as soil-only controls, where we measured respiration rates of soils for comparison to the measurements from trays containing soil plus roots. One was located at the edge of the hardwood stand and the pine plantation, a second was located within the hardwood stand, and a third was located near the *C. canadensis* and *L. tulipifera* stand.

For each pair of trays per study tree, one of two root trays was treated with ZeroTol (BioSafe Systems, Hartford, CT USA), a broad-spectrum algaecide, bactericide and fungicide containing peroxyacetic acid (2%) and hydrogen peroxide (27.1%), to reduce the abundance of soil microbes and fungi in the root microbiome. The ZeroTol was applied every two weeks for the duration of the experiment, with each dose consisting of 350 mL of a 1% solution, which was enough to saturate the soil. The second tray of each pair was treated with 350 mL of water to reduce any soil moisture effects of the ZeroTol application. Surface leaf litter was removed from each tray for each application of the ZeroTol or water; then leaf litter was replaced.

#### 2.2.1. Measurement of leaf functional traits

Leaf functional trait measurements were done to quantify aboveground plant economic strategies of the eight study species, which complemented root trait measurements. Leaf functional traits were measured in September 2019, before the onset of fall senescence. Five leaves per tree species (one per study individual) were collected, scanned, dried, and weighed. Scanned images were processed in ImageJ via R using code by Katabuchi (2015) to determine leaf area. Specific leaf area (SLA) was calculated by dividing leaf area by its dry mass. Leaf samples were ground to a fine powder using 15 mL sterile plastic vials and 1 mm stainless steel beads using the SPEX miniG 1600 (SPEX Sample Prep, Metuchen, NJ, USA). C and N concentrations of leaf ($C_{leaf}$ and $N_{leaf}$, respectively) tissues were determined using a Model 4010 Elemental Combustion System (Costech Analytical Technologies, Valencia, CA, USA) at Oak Ridge National Laboratory in Tennessee. Leaf phosphorus ($P_{leaf}$) concentrations in Kjeldahl digests were determined on a QuikChem 8500 analyzer (Lachat Instruments, Loveland, CO, USA) using Lachat Quikchem Method 13-115-01-1-B. Elemental concentrations are expressed as percent elemental dry matter.

#### 2.2.2. Measurements of specific root respiration ($R_r$) and root system functional traits of excised root systems

On three dates, during the spring and summer of 2020 (March 26, May 20, and June 24), we measured specific respiration rates of excised root systems ($R_r$) for all study species. Root material was traced out and excavated from five trees for all studied species, being careful to keep each root system intact to its finest, first-order roots. Trees from which root systems were harvested were not those with the *in-situ* root trays but were nearby comparable individuals (*i.e.*, of the same size). Root material was thoroughly washed, removing all soil. In some instances (*e.g.*, *Fagus*, *Oxydendrum*, and *Pinus* roots), ectomycorrhizal hyphae were left attached to roots if removing them would damage the root system. Root material was delineated into entire root systems containing at least three root orders, including the finest first-order roots (as described in McCormack et al., 2015) by cutting root systems off at the fourth-order transportive root. Root systems were placed in a Walz WK-G1 respiration chamber set to 25 °C. The Walz respiration chamber was attached to the

Li-6800, which fed air into the chamber and recorded the gas exchange measurements. Stability criteria for these measurements were $\Delta CO_2$, slope < 0.25, and standard deviation < 0.1 μmol mol$^{-1}$ and $\Delta H_2O$ slope < 0.25, and standard deviation < 0.1 μmol mol$^{-1}$ assessed over a 20 s interval.

Following $R_r$ measurements, root systems were scanned using a double-sided optical scanner (Epson Perfection V800, Epson America Inc.) at high resolution (1400 dpi) in black and white. Roots were then dried in paper bags at 60 °C for several days and then weighed. Scanned root images were analyzed using WinRHIZO (2016 version, Regent Instruments, Quebec, Canada). WinRHIZO measures root length, area, average diameter, volume, and architectural parameters of root systems. Specific root length (SRL) and specific root area (SRA) were calculated by dividing root length and area by root system dry mass. RTD was calculated as the ratio of the root system dry mass to its volume. Root samples were ground to a fine powder using 15-mL sterile plastic vials and 1 mm stainless steel beads using the SPEX miniG 1600 (SPEX Sample Prep, Metuchen, NJ, USA). C and N concentrations of root tissues ($C_{root}$ and $N_{root}$, respectively) were determined using a CE Flash 1112 Elemental Analyzer (Thermo Fisher, Waltham, MA USA) using standard C-N sample protocols at the Blue Carbon Analysis Lab at Florida International University in Miami, Florida.

### 2.3. Field measurements of $R_s$

From July 2019 to May 2020, we measured gas exchange of the root trays using a custom chamber (see methods S1) attached to an Li-6800 portable photosynthesis system (Li-COR Inc., Lincoln, NE USA). Measurements were taken bi-weekly from June until November 2019, wherein measurements were done monthly for the winter months until March 2020. For each of the 80 root trays and the six soil-only controls, leaf litter was removed, and the tray was placed in the custom gas exchange chamber attached to the Li-6800. The chamber was closed and sealed around the root system at the transportive root, which was still attached to the tree, using plumber's putty (Oatey, Cleveland, OH USA). The air pump of the Li-6800 was set to high, resulting in a flow rate of between 1400 and 1500 μmols s$^{-1}$. Accounting for the volume of the chamber, the time constant (τ) of the gas exchange system, or the chamber volume to flow rate ratio, was about 260 s, meaning that the air in the chamber could completely turn over in that time. Therefore, we set the following stability criteria to be evaluated over a 60-second period: relative humidity of the chamber, slope < 0.5% and standard deviation < 1%, and respiration rate, slope, and standard deviation both < 1 μmol m$^{-2}$ s$^{-1}$. Once stability was reached, the data point was logged.

During each root tray measurement, soil moisture and temperature of the top 5 cm of soil were measured. Soil moisture was measured with the SM150T soil moisture sensor with 5.1 cm measurement rods (from Delta T Devices Ltd. Cambridge, UK), and soil temperature was measured with a digital thermometer (accuracy 0.3 °C, Fisherbrand Traceable Flipstick thermometer, Thermo Fisher, Waltham, MA). While root trays were in the gas exchange chamber, three measurements were taken in each of the three cardinal directions opposite the origin of the plant root and averaged. Root trays were collected on May 28, 2020, by cutting root systems from trees. Trays containing root systems and soil were air dried for one week to facilitate soil separation from root systems. Root systems were removed from the trays, washed, rehydrated, and assessed for root system health. Root systems from the *in-situ* root trays were scanned in the same manner as roots used for $R_r$ measurements, using a double-sided optical scanner (Epson Perfection V800, Epson America Inc.) at high resolution (1400 dpi) in black and white, and dried at 60 °C for several days then weighed. The root system scans were analyzed using WinRHIZO (2016 version, Regent Instruments, Quebec, Canada) as described above. The total soil dry mass was weighed for each tray, and soils were sieved using sterile 1 mm mesh before laboratory analyses. Soil samples were taken from sieved and homogenized tray soil for further processing using sterile methodologies – 10 g for nutrient pool analyses and 80 g for sequencing; samples meant for sequencing were frozen.

### 2.4. Laboratory analyses of soils

Soil carbon pools reflect the amount of recalcitrant vs. labile carbon, which are a function of decomposition and activity of plant-root microbial associations (Condron et al., 2010; Rossi et al., 2020; Trumbore, 2006), and soil nitrogen pools indicate soil microbial abundance and metabolic activity (Brookes et al., 1985; Insam, 2001). At the end of the experiment, soil carbon and nitrogen pools, including soil microbial biomass carbon (MBC) and microbial biomass nitrogen (MBN), were measured for all trays (including soil-only controls) using soil chloroform fumigation extraction (Brookes et al., 1985, see Methods S3). To quantify communities of soil heterotrophic microbes in the trays, soil bacterial 16 s, and fungal ITS was extracted and sequenced (see method S4). Microbial sequences were processed with QIIME 2 v2020.2 platform (Bolyen et al., 2019). Paired sequences were demultiplexed and quality filtered (denoised, dereplicated, chimera filtered, and pair-end merged) and processed in Sequence Variants (SVs) with the demux and dada2 plugins (Estaki et al., 2020). Taxonomy was assigned using a pre-trained Naive Bayes classifier based on the SILVA database (Pruesse et al., 2012) trimmed to the 515F/806R primer pair for 16S reads and the UNITE database (Nilsson et al., 2018) for ITS2 reads. Unassigned sequences, mitochondrial, and chloroplast sequences were removed. Sequence variant-based richness and Shannon diversity were calculated with the QIIME package. Bray-Curtis beta-diversity was calculated with the phyloseq package (McMurdie and Holmes, 2013).

#### 2.4.1. Statistical analyses – traits, $R_r$, and soils

We tested for statistical differences in leaf and root functional traits of the excised root systems, including tissue elemental concentrations, using single-factor analysis of variance (ANOVA) and a Tukey test to determine which species were distinct from one another. Similarly, ANOVA was used to examine differences in soil C (TC, DOC, MBC) and N pools (TN, DN, MBN) from the soil chloroform extractions and differences in bacterial 16 s and fungal ITS richness and Shannon diversity. ANOVA models were fitted considering effects by species, treatment, collection area (as explained above in the study area description, see Fig. S1), and any possible interactions between those three factors (see methods S2). Lastly, we examined the factors affecting differences in tray soil bacterial and fungal community composition using permutational multivariate analysis of variance (PERMANOVA). Collection area, tree species, treatment, and interaction terms between treatment and tree species and treatment and collection area were considered.

Additionally, for each of the three measurements (March, May, and July) and their average, we tested for differences between $R_r$ among species again using single factor ANOVAs, followed by a Tukey test. A principal components analysis (PCA) was used to characterize the root functional trait space for the eight study species. Ten root functional traits were used: root system average diameter, length, surface area, tip abundance, SRL, SRA, specific root tip abundance (SRTA), RTD, and root tissue C and N concentrations. Species average root trait values (from 15 entire root systems each) were scaled and centered and then used for PCA. To examine relationships between the root functional trait space and specific respiration rates (*i.e.*, research question 1), average $R_r$ rates (measured from the same 15 entire root systems per species over three separate sampling periods, Table 2) were regressed (ordinary least squares regression) against the first two PC axes.

#### 2.4.2. Statistical analyses – Modeling the contribution of $R_r$ to $R_a/R_s$

To relate $R_r$ measurements to the *in-situ* root trays, we used the $Q_{10}$-temperature relationship of Palta and Nobel (1989, Atkin et al., 2000, Fig. S2). Average $R_r$ measured at 25 °C (Table 2) was used in combination with the $Q_{10}$-temperature function of Palta and Nobel (1989) via Atkin et al. (2000) to create $R_r$-temperature response curves for each

species. More specifically, the $R_r$ measurements from excised root systems determined the elevation of the $R_r$-temperature relationship, and we use the assumption of $Q_{10}$-temperature variation on $R_r$ to construct the shape of the $R_r$-temperature curve, which was identical for all species (Fig. S2). Then, for each tray, rates of *in-situ* root system respiration ($R_a$) at soil temperature were calculated from the $R_r$-T relationship by species, accounting for fine root system biomass, as measured at the end of the experiment. We found it best to model $R_s$ and examine the contribution of $R_a$ to $R_s$ using mass-based fluxes because this allowed us to work with raw fluxes of $CO_2$ (*i.e.*, nmol $s^{-1}$) having accounted for variation in root biomass and soil dry mass between trays. We also completed our analyses with area-based fluxes, and our results were qualitatively similar, but area-based $R_s$ created difficulty interpreting results because root material was measured on a per-mass basis. It is unclear if the shallow depth of the root tray (2 in.) affected area-based inferences. Thus, $R_r$ at the soil measurement T (in nmol $g^{-1}$ $s^{-1}$) was multiplied by the amount of root biomass per tray to get mass-based $R_a$. $R_s$ (the sum of $R_a$ and $R_h$, as the emergent measurement taken with the respiration chamber) was calculated as a mass-based flux using formulae for mass-based $CO_2$ fluxes developed by Li-Cor and dry mass of soil for each tray.

A separate PCA was done using the traits from root systems of the *in-situ* trays. The PCA used data from individual root systems on the same traits listed above (*i.e.*, for the PCA of excised root systems) except for $N_{root}$ and $C_{root}$. We modeled the $R_a/R_s$ ratio (*i.e.*, the fraction of autotrophic, root-derived respiration to total soil respiration) using a linear mixed-effects model (*i.e.*, gaussian error with identity link function). $R_a/R_s$ values were log-transformed to improve their normality. We explored including fixed effects for measurement date, root functional trait principal components 1 and 2 (from the PCA using traits from root systems housed in the root trays), treatment (*i.e.*, control vs. ZeroTol trays), soil moisture, soil temperature, mycorrhizal type (*i.e.*, AM vs. ECM hosts) and species identity and random intercept terms for species, root tray, and root tray nested within species. The 'step' function was used to find the best-fitting mixed-effects models, which uses backward model section on the random and fixed parts of the model (in that order) based on AIC. The best-fitting model included fixed effects for each sampling date. Model coefficients from the best-fitting model were estimates using restricted maximum likelihoods. Analyses were done using R v.4.0.3 (R Core Team, 2020) and made use of the lme4 (Bates et al., 2015), lmerTest (Kuznetsova et al., 2017), and sjPlot (Lüdecke, 2018) packages.

## 3. Results

### 3.1. Functional variation among study species

Root functional traits varied considerably among species, demonstrating that the eight species studied represented a wide range of root functional strategies. SRL varied 6 m $g^{-1}$ among the eight study species, ranging from about 3 m $g^{-1}$ for *L. styraciflua* to about 9 m $g^{-1}$ for *C. canadensis* (Table 1). Average $C_{root}$ concentrations varied little among species ranging from about 41 to 43 %, while $N_{root}$ varied up to 0.85% and was greatest for *C. canadensis* at 1.64%. SLA ranged from about 7 $m^2$ $kg^{-1}$ for *P. taeda* to 28 $m^2$ $kg^{-1}$ for several species including *N. sylvatica*. $C_{leaf}$ varied more than $N_{leaf}$ or $P_{leaf}$ concentrations, fluctuating up to 5% among the six study species in contrast to about 1% and 0.03% for $N_{leaf}$ and $P_{leaf}$, respectively. All in all, root and leaf functional variation among taxa showed that the eight species selected range in resource-use strategies, both above- and belowground.

The differences in the multivariate root functional trait space among a greater suite of root traits were summarized in a PCA (Fig. 1A), which used species average functional trait values (from 15 excised entire root systems) for ten root functional traits. The first two axes of the PCA explained 83.2% of the root functional variation among the eight study species. Principal component 1 (PC1 in Fig. 1A) depicts a root length ($r = -0.42$) and diameter ($r = 0.40$) tradeoff. In contrast, component 2 (PC2) is directly related to high $N_{root}$ ($r = -0.52$) and SRA ($r = -0.58$), with RTD ($r = 0.38$) trading off with these two traits, although weakly and not directly. Thus, the PCA adequately characterized functional variation in root morphologies among species, justifying regression with $R_r$ rates.

### 3.2. Specific root respiration rates – Variation among species and with root functional traits

Specific root respiration ($R_r$) rates were variable over time and among species (Table 2). There was a considerable variation in $R_r$ over the spring to summer months when excised root systems were collected and measured. Variation in measured $R_r$ over this time was not

**Table 1**
Leaf and root functional trait values for eight temperate tree species in the study. Specific leaf area (SLA) and leaf tissue elemental concentrations are averages (±standard errors) from 5 leaves of each species collected before fall leaf senescence in 2019. Specific root length (SRL), average root system diameter (D) and root tissue elemental concentrations are averages (±standard errors) for each species from 15 root systems excavated during the spring and summer of 2020. Asterix notation for statistical significance of F-statistics (ANOVA) is as follows: $*p < 0.05$, $**p < 0.01$, $***p < 0.001$, otherwise non-significant. Post-hoc Tukey HSD pairwise comparison groupings are denoted with letters.

| Species | Leaf traits | | | | Root traits | | | | |
|---|---|---|---|---|---|---|---|---|---|
| | SLA ($m^2$ $kg^{-1}$) | $C_{leaf}$ (%) | $N_{leaf}$ (%) | $P_{leaf}$ (%) | D (mm) | SRL (m $g^{-1}$) | RTD (g $cm^{-3}$) | $C_{root}$ (%) | $N_{root}$ (%) |
| *Fagus grandifolia* L. | 26.12 ± 1.71$^{C}$ | 45.66 ± 0.23$^{ABC}$ | 2.09 ± 0.03$^{D}$ | 0.100 ± 0.002$^{B}$ | 0.52 ± 0.01$^{A}$ | 5.17 ± 0.32$^{ABC}$ | 0.95 ± 0.04$^{D}$ | 41.51 ± 1.03$^{A}$ | 0.80 ± 0.05$^{A}$ |
| *Oxydendrum arboreum* (L.) DC. | 23.77 ± 1.13$^{C}$ | 45.41 ± 0.36$^{AB}$ | 1.77 ± 0.07$^{CD}$ | 0.112 ± 0.001$^{D}$ | 0.55 ± 0.02$^{A}$ | 5.88 ± 0.48$^{ABC}$ | 0.80 ± 0.04$^{CD}$ | 41.73 ± 0.47$^{A}$ | 1.11 ± 0.14$^{AB}$ |
| *Liquidambar styraciflua* L. | 14.51 ± 0.40$^{B}$ | 46.87 ± 0.34$^{BC}$ | 1.59 ± 0.03$^{BC}$ | 0.111 ± 0.002$^{C}$ | 0.88 ± 0.04$^{B}$ | 3.20 ± 0.31$^{A}$ | 0.58 ± 0.02$^{B}$ | 41.52 ± 0.91$^{A}$ | 0.79 ± 0.07$^{A}$ |
| *Acer rubrum* L. | 26.37 ± 0.63$^{C}$ | 46.35 ± 0.20$^{BC}$ | 1.56 ± 0.02$^{BC}$ | 0.113 ± <0.001$^{CD}$ | 0.51 ± 0.02$^{A}$ | 8.22 ± 1.27$^{CD}$ | 0.73 ± 0.06$^{BC}$ | 41.85 ± 1.64$^{A}$ | 0.79 ± 0.07$^{A}$ |
| *Nyssa sylvatica* Marshall | 27.67 ± 0.71$^{C}$ | 43.92 ± 0.31$^{A}$ | 1.38 ± 0.08$^{B}$ | 0.095 ± 0.002$^{B}$ | 0.51 ± 0.02$^{A}$ | 7.06 ± 0.97$^{BCD}$ | 0.82 ± 0.06$^{CD}$ | 43.25 ± 0.56$^{A}$ | 0.92 ± 0.04$^{A}$ |
| *Cercis canadensis* L. | 17.68 ± 1.12$^{B}$ | 47.34 ± 0.49$^{C}$ | 1.82 ± 0.05$^{CD}$ | 0.130 ± 0.002$^{E}$ | 0.45 ± 0.01$^{A}$ | 9.06 ± 0.67$^{D}$ | 0.77 ± 0.06$^{BD}$ | 42.24 ± 1.18$^{A}$ | 1.64 ± 0.11$^{C}$ |
| *Pinus taeda* L. | 6.86 ± 0.19$^{A}$ | 50.32 ± 0.27$^{D}$ | 1.02 ± 0.03$^{A}$ | 0.084 0.002$^{A}$ | 0.82 ± 0.06$^{B}$ | 4.18 ± 0.55$^{AB}$ | 0.58 ± 0.03$^{B}$ | 42.87 ± 0.98$^{A}$ | 0.95 ± 0.11$^{A}$ |
| *Liriodendron tulipifera* L. | 17.73 ± 1.35$^{B}$ | 46.99 ± 0.68$^{BC}$ | 1.98 ± 0.15$^{D}$ | 0.132 ± 0.002$^{E}$ | 1.04 ± 0.03$^{C}$ | 4.38 ± 0.36$^{AB}$ | 0.29 ± 0.02$^{A}$ | 40.85 ± 0.60$^{A}$ | 1.41 ± 0.07$^{B}$ |
| $F_{species}$ | $F_{(7,32)}$ = 49.52*** | $F_{(7,32)}$ = 22.92*** | $F_{(7,32)}$ = 24.37*** | $F_{(7,32)}$ = 87.98*** | $F_{(7, 113)}$ = 47.57*** | $F_{(7, 113)}$ = 8.53*** | $F_{(7, 113)}$ = 20.71*** | $F_{(7, 43)}$ = 0.67* | $F_{(7, 43)}$ = 16.11*** |

**Table 2**
Average (±standard error) specific root respiration rates for eight temperate tree species (ordered from least to greatest average $R_r$). Respiration was measured at 25 °C for excised entire root systems (with ≥ three root orders) using a Li-6800 portable gas exchange system attached to a Walz 3010-GWK1 chamber. Three replicates of five root systems per species were measured during each measurement date in the spring and summer of 2020. Averages are given in the rightmost column, which were used to estimate tissue respiration rates for *in-situ* root trays using the temperature-response curves constructed via the $Q_{10}$-temperature function from Palta and Nobel (1989, see methods, Fig. S2).

| Species | Measurement 1 3/26/2020 (n = 5) nmol $g^{-1}$ $s^{-1}$ | Measurement 2 5/20/2020 (n = 5) nmol $g^{-1}$ $s^{-1}$ | Measurement 3, 7/24/2020 (n = 5) nmol $g^{-1}$ $s^{-1}$ | Average (n = 15) nmol $g^{-1}$ $s^{-1}$ |
|---|---|---|---|---|
| *Fagus grandifolia* L. | $3.02 \pm 0.28^{A}$ | $2.64 \pm 0.60^{A}$ | $1.81 \pm 0.31^{A}$ | $2.49 \pm 0.26^{A}$ |
| *Oxydendrum arboreum* (L.) DC. | $3.74 \pm 1.54^{A}$ | $3.00 \pm 0.36^{A}$ | $1.94 \pm 0.12^{A}$ | $2.89 \pm 0.53^{A}$ |
| *Liquidambar styraciflua* L. | $2.03 \pm 0.64^{A}$ | $4.33 \pm 0.92^{AB}$ | $2.51 \pm 0.29^{A}$ | $2.96 \pm 0.45^{A}$ |
| *Acer rubrum* L. | $2.18 \pm 0.18^{A}$ | $3.58 \pm 0.66^{A}$ | $4.45 \pm 0.80^{A}$ | $3.41 \pm 0.41^{A}$ |
| *Nyssa sylvatica* Marshall | $5.66 \pm 0.95^{AB}$ | $3.18 \pm 0.58^{A}$ | $1.79 \pm 0.17^{A}$ | $3.54 \pm 0.55^{A}$ |
| *Cercis canadensis* L. | $4.51 \pm 0.72^{AB}$ | $5.42 \pm 1.15^{AB}$ | $2.50 \pm 0.28^{A}$ | $4.14 \pm 0.54^{A}$ |
| *Pinus taeda* L. | $5.57 \pm 0.74^{AB}$ | $4.34 \pm 0.96^{AB}$ | $3.75 \pm 0.16^{A}$ | $4.56 \pm 0.33^{A}$ |
| *Liriodendron tulipifera* L. | $10.02 \pm 2.66^{B}$ | $7.17 \pm 0.68^{B}$ | $9.94 \pm 1.68^{B}$ | $9.04 \pm 1.05^{B}$ |
| | $F_{(7,32)} = 4.509$** | $F_{(7,32)} = 4.375$** | $F_{(7,32)} = 15.84$*** | $F_{(7,113)} = 13.95$*** |

systematic in that some species showed an increase in $R_r$ from spring to summer (*e.g.*, *A. rubrum*), while others showed a decrease (*e.g.*, *P. taeda*). Despite this, statistical differences in $R_r$ among species emerged for each measurement, with patterns among species being qualitatively consistent. Thus, the average $R_r$ rates over the three measurements are likely the best representation of the intraspecific variation in $R_r$ over the study period. *L. tulipifera* had the greatest average $R_r$, being at least double that of the remaining seven species, with average $R_r$ rates of the remaining seven species all contained in the same Tukey HSD grouping (Table 2).

The regression of $R_r$ rates on PC1 (*i.e.*, the tradeoff in root length and diameter) was not statistically significant, yet a slight trend was evident (Fig. 1B; slope $p = 0.25$). However, the regression of $R_r$ rates on PC2 (*i.e.*, the $N_{root}$ – RTD axis of root functional variation) was statistically significant (Fig. 1C, slope $p < 0.01$). Thus, species with higher $N_{root}$ typically had higher $R_r$ rates. Because $N_{root}$ was aligned almost perfectly to the negative side of PC2, we can interpret the slope of the regression in terms of $N_{root}$ in conjunction with species-average root trait covariation among the eight species, meaning that within the functional trait space respiration rates roughly decline 1 nmol $g^{-1}$ $s^{-1}$ per % decrease in $N_{root}$ (Fig. 1C). The direct relationship between $R_r$ and $N_{root}$ showed the relationship to be steeper, yet more variable for individual root systems, wherein $R_r$ rates declined 3.6 nmol $g^{-1}$ $s^{-1}$ per % decrease in $N_{root}$ ($p < 0.001$, $R^2 = 0.14$, Fig. S3).

### 3.3. Soil bacterial and fungal communities – The effect of the ZeroTol treatments on in-situ root trays

Overall, the application of the algaecide-bactericide-fungicide ZeroTol did not completely sterilize the soils. While the treatment had only a minor, marginally-significant effect on bacterial 16S Shannon diversity (Table S2, Fig. S4, $F_{(1,82)} = 1.76$, $p = 0.19$) or alpha richness ($F_{(1,82)} = 2.61$, $p = 0.11$), the effect on 16S community composition was significant (Table S3, $F_{(1,83)} = 1.96$, $p = 0.19$, Fig. S5). The PERMANOVA showed that the collection area overwhelmingly influenced soil bacterial 16 s community composition, explaining 15 times the compositional variation explained by treatment and over 3 times the variation explained by tree species (Table S3). Including effects for species or collection area or their interactions with treatment did not change the ANOVA results for bacterial richness or Shannon diversity (*i.e.*, lead to an increase in the treatment effect). Similarly, interaction terms between species and treatment and collection area and treatment in the PERMANOVA for bacterial 16 s were not significant (Table S3). The Zerotol treatment led to a decrease in microbial (*i.e.*, bacterial) biomass in the root trays as evidenced by a decrease in MBN concentrations ($F_{(1,75)} = 31.66$, $p < 0.001$; Fig. 2A, Table S4).

Fungal ITS richness and diversity were similarly unaffected by the ZeroTol treatment, although in the trays of some species, there was an increase in the relative abundance of Basidiomycota at the expense of Ascomycota (Fig. 2B, Table S2). The PERMANOVA showed that again collection area had the strongest influence on soil fungi community composition, but treatment and species effects were slightly stronger

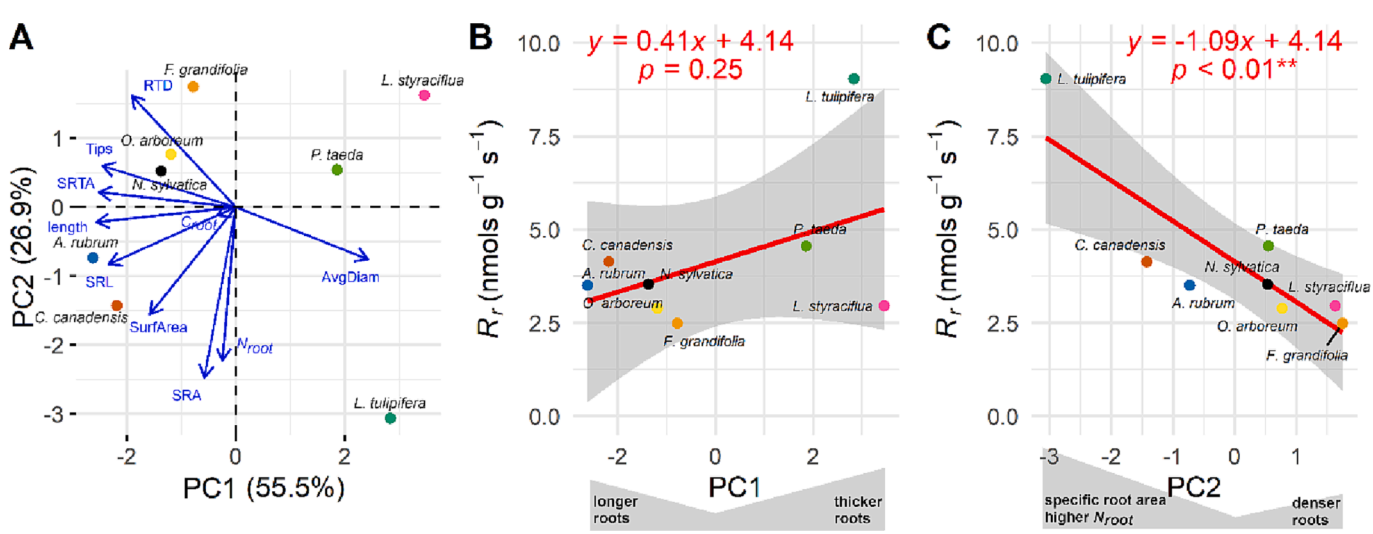


**Fig. 1.** **A**) Principal components analysis of species mean root functional traits for eight temperate tree species (where point color matches Figs. 2 & 3). **B** and **C**) linear regressions of $R_r$ and principal component axes. Regression equations and *p*-values for regressions slopes are shown. Gray triangular bars below the x-axes show the relative magnitude of functional trade-offs for the most strongly correlated functional traits and each PCA axis.

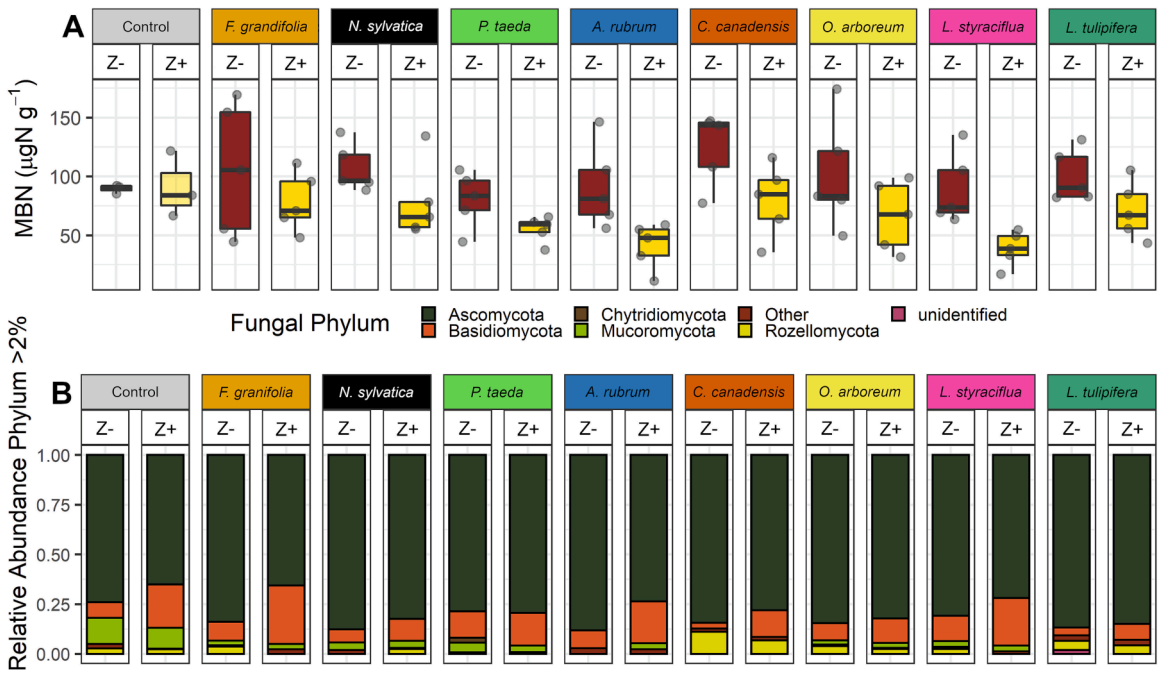


**Fig. 2.** The effect of the algaecide-bactericide-fungicide treatment on the soil microbiome. **A**) Microbial biomass nitrogen (MBN) concentration in soils by species and treatment. Generally, MBN was lower in ZeroTol-treated trays (Z + ). **B**) The relative abundance of the most-prevalent fungal phylas. Overall, there was an increase in fungal abundance (*i.e.*, read number), driven by an increase in Basidiomycete fungi in the ZeroTol-treated trays. For a similar graphic showing little change in relative abundances of bacterial phyla by treatment or among species see Figure S5.

than for bacterial composition, with significant interactions with treatment (Table S3). Except for the difference in MBN among treatments, differences in soil C and N pools were not found between treatments but did differ among species (Fig. S5, see Table S4 for *F*-statistics). For example, total and dissolved organic carbon differed statistically among species (TC: $F_{(9,75)} = 3.05$, $p < .01$; DOC: $F_{(9,75)} = 2.62$, $p < 0.05$) although Tukey HSD groupings showed no difference among species. The same trend was evident in soil total and dissolved nitrogen (TN: $F_{(9,75)} = 2.08$, $p < 0.05$; DN: $F_{(9,75)} = 1.89$, $p < 0.10$; Table S4, Fig. S6).

A non-metric multidimensional scaling (NMDS) ordination of root tray soil bacterial and fungal communities showed that soil microbial composition was primarily structured by collection area (Fig. S7), despite differences in the ANOVA analysis for collection area only being detectable for fungal ITS sequences and not 16S bacterial sequences (Fig. S5). Indeed, the clustering of fungal communities by collection in the NMDS was more distinct than the clustering of the bacterial communities; however, in both the fungal and bacterial composition, three distinct assemblages emerged, with communities being similar by forest area (see Fig. S1 for map).

### 3.4. Estimating the contribution of $R_a$ to $R_s$ for the in-situ root trays

Total soil surface $CO_2$ efflux from the *in-situ* root trays ($R_s$) ranged from 0.30 to 11.99 μmol m$^{-2}$ s$^{-1}$ (11.74 to 475.42 nmol kg$^{-1}$ s$^{-1}$) and averaged 2.21 ± 0.04 μmol m$^{-2}$ s$^{-1}$ (82.47 ± 1.51 nmol kg$^{-1}$ s$^{-1}$) over the 11-month study period (Fig. 3). For the soil only control trays (*i.e.*, those lacking roots, R-), total soil surface $CO_2$ efflux ranged from 0.48 to 7.13 μmol m$^{-2}$ s$^{-1}$ (19.78 to 314.49 nmol kg$^{-1}$ s$^{-1}$), averaging 1.73 ± 0.11 μmol m$^{-2}$ s$^{-1}$ (67.85 ± 4.61 nmol kg$^{-1}$ s$^{-1}$) (Fig. S8). Accounting for variation in the amount of soil among trays, the total raw $CO_2$ flux from trays ranged from 14.43 to 583.66 nmol s$^{-1}$, with a mean value of 107.46 ± 2.00 nmol s$^{-1}$ and with 95% of observations measuring between 26.09 and 317.94 nmol s$^{-1}$ (Fig. S8A).

Using some assumptions about how $R_r$ varies with temperature via the $Q_{10}$-temperature function of Palta and Nobel (1989; Fig. S2; Atkin et al., 2000), we separated the $R_s$ measurements from the *in-situ* root trays into $R_a$ and $R_h$ components. The partitioning of $R_s$ was best done using mass-based measurements of soil $CO_2$ efflux because $R_a$ was calculated on a per root-system dry mass basis using $R_r$ for the entire root systems housed in the *in-situ* root trays. $R_a$ varied from 0.15 to 18.04 nmol s$^{-1}$, averaging 2.18 ± 0.06 nmol s$^{-1}$ (Fig. S8B) and with 95 % of measurements being between 0.28 and 7.57 nmol s$^{-1}$ (Fig. S8B). The 95% confidence interval for the contribution of root respiration to the total $CO_2$ efflux from the root-soil tray system ($R_a/R_s$) was 0.27% to 12.86%.

### 3.5. Effects of root functional strategies on $R_a/R_s$

Our second research question inquired if differences in root functional traits could explain variation in belowground $CO_2$ efflux. Moreover, given the differences in $R_r$ among species (Table 2, Fig. 1), we could ask which axis of root functional trait space best relates to species-driven variation in $R_a/R_s$? Root functional differences were determined by a second PCA using root trait data from the root systems housed in the trays; this second PCA (Fig. 4A) was similar to the first PCA (Fig. 1A), which used data from the excised root systems, in that SRA ($r = 0.53$) roughly traded off with RTD ($r = -0.74$) on axis 2, being organized orthogonally to SRL and the number of root tips (both $r = -0.42$). The first two principal components accounted for the vast majority (nearly 83%) of the functional trait variation among the root systems from the trays. SRL and the root tip abundance were the largest contributors to PC1, each explaining about 17% of its variation (although PC1 was also associated with total root length, root system surface area, SRA, SRTA, and average diameter). In contrast, RTD was the largest contributor to PC2, explaining about 54% of its variation (Fig. 4A). Thus, root systems that had higher SRL, root tip abundance, and separately, greater RTD had greater $R_a/R_s$ . Moreover, $R_a/R_s$ decreased as root system SRL, tip abundance, and RTD decreased (Fig. 4B, Fig S10).

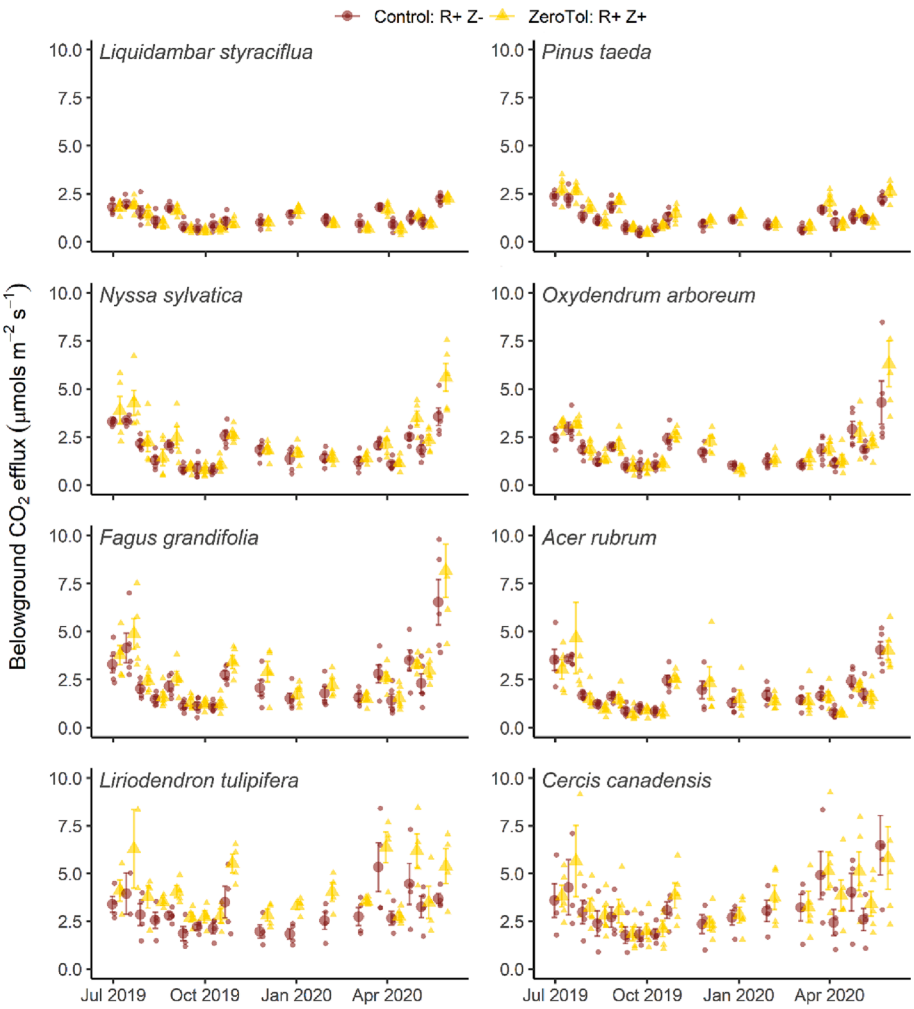


**Fig. 3.** Rates of belowground $CO_2$ efflux ($R_s$, area-based in μmol $m^{-2}$ $s^{-1}$) for *in-situ* root trays for eight temperate tree species from July 4, 2019, to May 26, 2020, by tree species. Colors correspond to treatments, with yellow for the ZeroTol-treated trays and brown for controls. Large points represent mean rates per treatment per species (n = 5), with intervals showing standard errors, while smaller points show the individual measurements for each tray. Panels are organized by collection area with the top two panels, the middle four panels, and the bottom two panels belonging to the same collection areas (see Figure S1).

### 3.6. Variation in $R_a/R_s$ – treatment, seasonal, soil moisture, and soil temperature effects

Differences in area-based soil $CO_2$ efflux rates between the control and ZeroTol-treated trays of a sampled tree ranged from 8.31 μmol $m^{-2}$ $s^{-1}$ greater to 4.65 μmol $m^{-2}$ $s^{-1}$ less in the treated trays relative to control trays, with 95% of observations being between 2.61 μmol $m^{-2}$ $s^{-1}$ greater and 1.42 μmol $m^{-2}$ $s^{-1}$ less, respectively (Fig. 3). There was a tendency for area-based soil $CO_2$ efflux rates to be greater in treated than in control trays, especially for *F. sylvatica*, *P. taeda*, and *L. tulipifera* (Fig. 3, Fig. 5B). However, when soil and root system masses were incorporated, differences in mass-based $R_s$ between treatments were subtle, indicating the treatment did not induce the desired reduction in $R_h$ (Fig. S8).

The mixed-effects model (Table S5, Fig. S9) showed that temporal fluctuations in $R_a/R_s$ dominated the variability in the dataset. There was a clear and significant increase in $R_s$ just before leaf senescence and shed in the fall months (*i.e.*, September and early October) (Fig. 3, Fig. S12). The mixed-effects models showed that at least some of the increase in $R_s$ during this time was related to $R_a$, as the $R_a/R_s$ fraction increased (Fig. 5A). Mean soil moisture ranged from about 11% to about 30% and tended to be higher in the winter and spring months relative to the fall (Table S6). Average soil temperatures fluctuated between 6 and 26 °C and were lowest from November until the beginning of March (Table S6). After accounting for temporal fluctuations in $R_a/R_s$, greater soil moisture reduced $R_a/R_s$ (β of −0.04, $p < 0.05$, Table S5, Fig. 5C, Fig. S11B), and warmer soil temperatures increased $R_a/R_s$ (β of 0.41, $p <$ 0.001, Table S5, Fig. 5D, Fig. S11C).

## 4. Discussion

### 4.1. Assumptions of the method and the analytical approach

Determining the $R_a$ contribution to $R_s$ for each *in-situ* root tray relies on several assumptions. First, we assumed that the biomass of the root systems is unchanged over time. Second, we assumed that root morphology is consistent over time. Third, we assume a universal temperature sensitivity of $R_r$ to model $R_a$, which was derived from the $Q_{10}$-temperature relationship for *Agave deserti* roots by Palta and Nobel (1989, see Atkin et al. 2000). Visual comparison of images of the root systems before their placement in the trays to the root system scans at the end of the experiment showed that generally, root systems changed little in morphological form and extent. In some cases, roots decreased in health or increased slightly in root tip abundance, yet most roots remained healthy despite not growing very much. There were no clear observational trends in root turnover based on pre-installation and post-harvest images across the 80 root systems studied. The assumption that the $Q_{10}$ values of $R_r$ do not vary much across species is supported by empirical evidence. For example, a recent study by Noh et al. (2020) found no difference in the $Q_{10}$ values of $R_r$ for temperate versus tropical seedlings (using eight species, four temperate and four tropical) grown between 16 and 32 °C. $Q_{10}$ values in that study ranged from 1.77 to 2.46 and averaged 2.15, which mirrors the range of $Q_{10}$ values we used to model $R_a$ (root system respiration at soil temperature for roots housed in

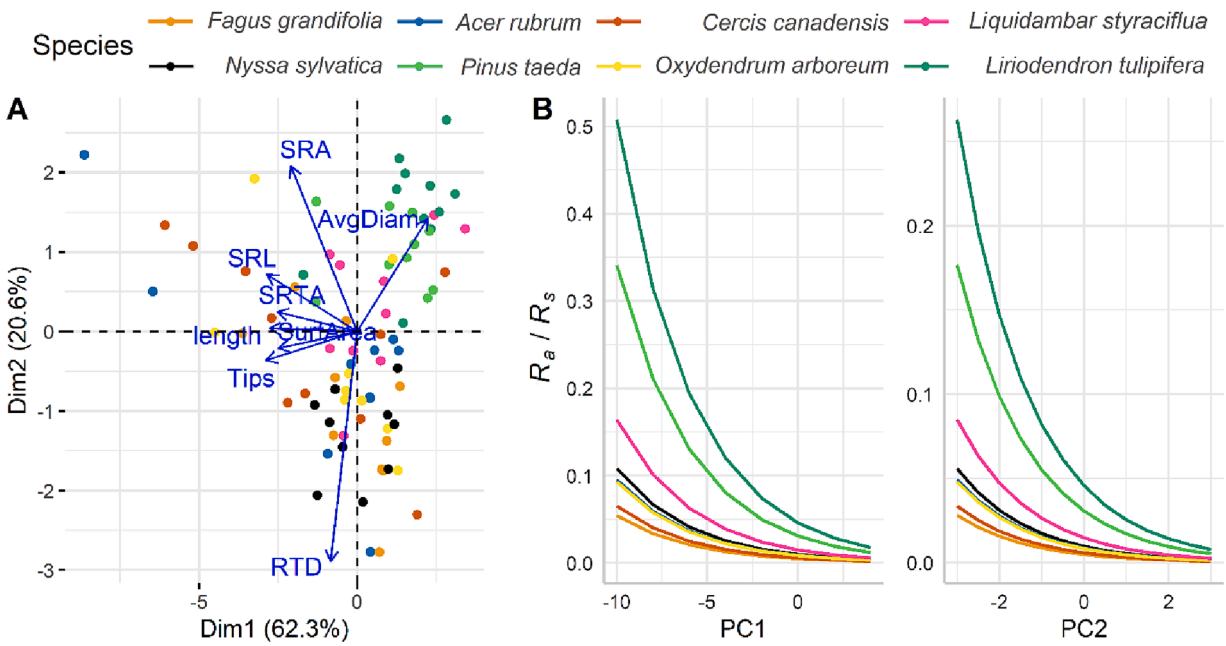


**Fig. 4.** **A**) Principal components analysis for root morphological traits of 80 entire root systems placed in *in-situ* root trays. Arrows show root trait variable loadings within the functional trait space, while individual points show locations of each root system within the root functional trait space. Points are colored by species (in correspondence with common names in Figs. 1-3). Abbreviations are: SRL – specific root length, SRA – specific root area, SRTA – specific root tip abundance, and RTD – root tissue density. SRL and root tip abundance (Tips) are loaded heaviest on PC1, and RTD is loaded heaviest on PC2. **B**) Best unbiased linear predictors of species loadings on PC1 and PC2 for $R_a/R_s$.

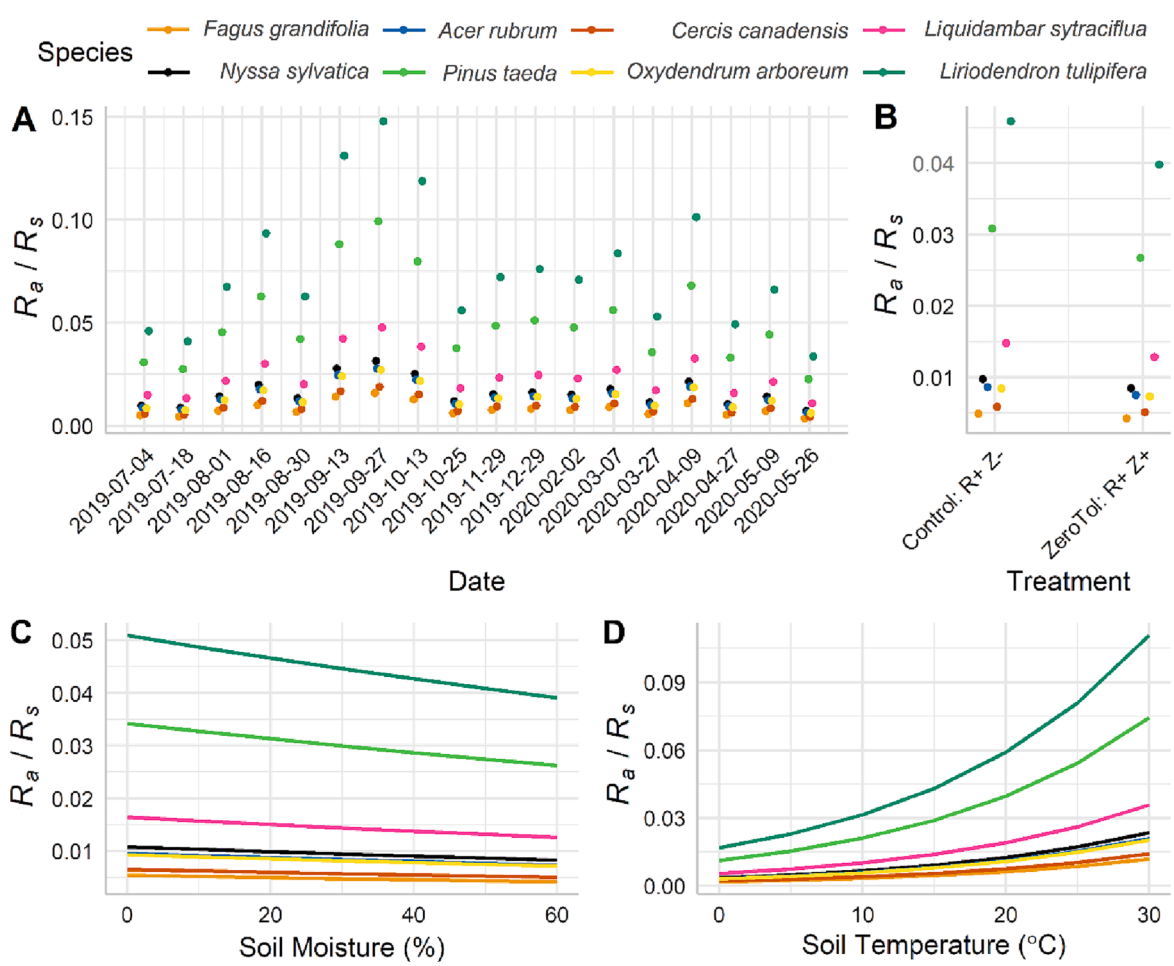


**Fig. 5.** Species-based best unbiased linear predictors for time (A), treatment (B) soil moisture (C) and soil temperature (D) on $R_a/R_s$.

the *in-situ* root trays) from $R_r$ (root tissue-specific respiration rates, see Fig. S2). Additionally, the temperature sensitivity of temperate tree $R_r$ (at least for *Acer saccharum* and *Pinus resinosa*) has been shown to be consistent (*i.e.*, not statistically different) among seasons, further supporting the use of a consistent $Q_{10}$-temperature relationship in $R_a$ models (Burton and Pregitzer, 2003).

### 4.2. Interpreting $R_r$ regarding tree species resource economics strategy

Specific root tissue respiration rates ($R_r$) have been demonstrated to scale with $N_{root}$ content and inversely with RTD, which oftentimes characterizes a functional tradeoff in root nutrient acquisition cost vs. tissue construction cost (Burton et al., 2002; Ceccon et al., 2016; Gao et al., 2021; Jia et al., 2013; Makita et al., 2015; Paradiso et al., 2019; Reich et al., 2008). $N_{root}$ reflects variation in species' ability to acquire soil N, which is a function of soil N availability and the myriad metabolic processes by which roots uptake and assimilate N. Variation in species' abilities to acquire and assimilate N informed our hypothesis about how root strategy, as indicated by root functional traits would relate to $R_r$; specifically, we questioned whether species with thicker root diameters, as a proxy for the conservative root strategy, had higher $R_r$.

Root functional trait data from the eight temperate tree species studied here, condensed nicely into two axes of variation, where root system diameter traded off with root system tip abundance to best characterize axis 1 and with $N_{root}$ ordinating almost directly in line with axis 2, and being somewhat inversely related to RTD. $R_r$ was positively but not significantly related to axis 1; however, $R_r$ had a significant negative relationship to axis 2. Thus, we confirm previous findings that $R_r$ scales with the RTD – $N_{root}$ tradeoff in root functional strategy. We found marginal support for the hypothesis that $R_r$ is positively related to root system diameter; however, this was mostly driven by the high $R_r$ for the thick-rooted *L. tulipifera*. Recent work has shown the root diameter-SRL axis of functional variation to be independent of the RTD – $N_{root}$ axis of functional variation across a wide range of plants from many biomes (Bergmann et al. 2020; Weigelt et al. 2021). Considering the taxa in this study, the root systems of *L. tulipifera*, *L. styraciflua*, and *P. taeda* have relatively few root tips per root system compared to the other five species in the study, and our results indicate that high root tip abundance likely leads to lower $R_r$. These results need to be tested and verified across more species.

### 4.3. Root functional strategy and its effect on $Ra/R_s$

Our second research question addressed whether variation in $R_r$ as a function of root morphology would translate to differences in the contribution of root respiration to total belowground $CO_2$ efflux from the *in-situ* root trays (*i.e.*, $R_a/R_s$). The hypothesis was that species with higher $R_r$ would contribute a more significant proportion of $R_a$ to $R_s$ and that the magnitude of the contribution might be modulated by mycorrhizal type. The contribution of $R_a$ to $R_s$ was positively related to root system acquisitiveness, as represented by the PCA axes of root system variation, with axis 1 most strongly representing variation in SRL and root tip abundance, and axis 2 representing RTD variability. Thus, the contribution of $R_a$ to $R_s$ decreased with decreasing SRL, root system tip abundance, and RTD.

We found no clear pattern of differences in $R_a/R_s$ with tree species mycorrhizal association type (*i.e.*, AM vs. ECM species, Fig. S12). $R_a$ may have been slightly higher for AM than for ECM trees, but any difference in $R_a$ was mirrored by $R_s$, making the $R_a/R_s$ ratio similar (Fig. S12). Tree mycorrhizal type was considered as a factor during the model fitting process, however, was excluded during model selection because of its lack of explanatory ability. This is likely a result of low sample sizes and little overlap in the root functional strategies of AM and ECM species. Among the eight species included in this study, we have thick and thin-rooted AM tree species, however, the two ECM taxa (*Fagus grandfolia* and *Pinus taeda*) have relatively narrow root diameters. Future work should consider a wider range of taxa across more variable root functional morphologies.

### 4.4. The effect of the ZeroTol treatment on tray soils and $R_s$

The ZeroTol treatments lysed bacteria which primed soil fungi in some cases (*i.e.*, accelerated the proliferation of fungi because of available nutrients related to dead bacteria), yet overall, the net effect on bacterial richness or diversity was slight and non-significant. Microbial N dropped as a result of repeated bi-weekly ZeroTol application to the soil surface, illustrating that bacterial biomass was reduced, but much less than intended, or as we have observed under laboratory conditions. Despite some reduction in bacterial biomass, $R_s$ rates from treated trays were not different from control trays (*i.e.*, those treated with water only, Fig. 3 & Fig. S8A), providing evidence for a compensatory dynamic between the contribution of bacterial and fungal $R_h$ to $R_s$, becuase of the increased abundance of certain fungal groups (*e.g.*, the Basidiomycota, Fig. 2).

Future studies that seek to sterilize soils should rely on more reliable methods (*e.g.*, gaseous chemical application, as opposed to liquid), which often use more potent and hazardous chemicals (*e.g.*, methyl bromide, chloroform, mercuric chloride, etc.). Despite the efficacy of many potent agents in sterilizing soils, there are often side effects on soil fertility (Trevors, 1996), which we wanted to avoid because of the effects that changes in soil nutrient availability can have on root growth and morphology.

### 4.5. Comparing measured $R_s$ fluxes with other studies – Interpreting temporal variation in $R_a/R_s$ over time

In a similar *Fagus sylvatica* forest in northeastern France, using area-based gas exchange methods on small plots with and without roots, Epron et al. (1999) found that root respiration accounted for 60% of the soil $CO_2$ efflux; total soil $CO_2$ efflux measured 1.74 μmol $m^{-2}$ $s^{-1}$, of which the root-associated portion was estimated to be about 1.06 μmol $m^{-2}$ $s^{-1}$. In the present study, we measured total $CO_2$ efflux to be around 2.17 (±0.04 standard error, n = 1537) μmol $m^{-2}$ $s^{-1}$; however, because we were working at the level of the individual entire root system (which contains three or more root orders), the amount of root biomass per unit soil area or volume was much less than what would occur in normal conditions. Hence, we estimated root respiration in the trays to be, on average, 2.04 nmols $g^{-1}$ $s^{-1}$ for root systems averaging 1.15 g dry mass, equaling 2.9 (±0.01 standard error) %. There was considerable temporal variation, and the contribution of root respiration to total soil $CO_2$ efflux peaked in the fall of 2019 (*i.e.*, August to September), contributing between 5.5 and 7.5% of total soil $CO_2$ efflux (Fig. 5). Although calculations of the contribution of $R_a$ to $R_s$ on a mass basis are not very common, our measurements for total $R_s$ are roughly comparable to those in the literature for similar forests, however $R_a$ estimates are low because the experimental design limited root presence to a single root system.

In temperate deciduous forests of the Northern hemisphere, temporal variability in the direct (via $R_a$) autotrophic contribution to $R_s$ peaks in the late fall (Edwards and Sollins, 1973; Yang and Wang, 2006). $R_a$ is related to tree growth rates and production and respiration rates ($R_r$) of many temperate tree species peaks in the fall (Yang and Wang, 2006, Abramoff and Finzi, 2016). Additionally, the increased litterfall during this time can lead to an increase in $R_s$ via effects on $R_h$ (Metcalfe et al., 2011; Raich and Tufekciogul, 2000). Our results provide support to the understanding that at least some of the increase in $R_s$ during the fall is related to increases in $R_r$. Empirically, across a variety of forest types, the autotrophic and heterotrophic components of $R_s$ have been shown to correlate to one another (Bond-Lamberty et al., 2004), as they are linked via labile C allocation and partitioning among the plant-soil system, which varies over time as trees modulate their aboveground to belowground carbon allocation (Chen et al., 2011; Chen et al., 2014; Metcalfe et al., 2011).

Many studies support our findings of the positive effects soil temperature on $R_a/R_s$ (Chen et al., 2011; Edwards and Sollins, 1973; Reichstein and Beer, 2008). $R_r$ is highly temperature dependent, increasing on average about 2 nmol $g^{-1}$ per 10 °C increase in soil temperature (Atkin et al. 2000). Soil temperature varied consistently with season in the temperate deciduous forest studied here, and plant metabolic activity slowed considerably in the cooler winter months when trees were leafless, which also likely indirectly affected $R_r$ and thus $R_a$ *in situ* due to reduced photosynthate (*i.e.*, carbon) supply to roots. The positive relationship between the contribution of $R_a$ to $R_s$ and increasing soil temperatures could also be a result of temperature-dependent metabolic process within soils and how roots interact with soil microhabitats to modulate the flow of air, water, and other resources through the soil matrix to facilitate microbial activity (*i.e.*, $R_h$) (Davidson and Janssens, 2006; Metcalfe et al., 2011). However, such relationships concerning the contribution of $R_a$ to $R_s$ with soil temperature may be equal in magnitude to effects produced by seasonal variability in liable carbon supply to roots (Bond-Lamberty et al., 2004; Chen et al., 2014). These competing drivers to variation of $R_a/R_s$ are difficult to separate due to their coupled occurrence during the cooler winter months in temperate forests where both carbon supply to roots and temperatures decrease.

### 4.6. Implications for ecosystem models: Root traits matter

Most ecosystem or terrestrial biosphere models include $R_s$ (belowground carbon flux) as a major component of system carbon loss (see summary table in Warren et al., 2015). $R_s$ is often modeled as a fraction of total gross primary productivity, which sometimes varies with the root biomass stock or root age; and within some models, $R_s$ magnitudes vary as it competes with other carbon sinks for photosynthate allocation. To our knowledge, such models have never included root functional traits such as SRL, RTD, or mycorrhizal type as potential modulators of $R_s$. In addition to temporal dynamics, our results show that species with acquisitive morphologies such as higher SRL and greater root tip abundance contribute a more significant percentage of $R_a$ to $R_s$. However, RTD, a trait associated with a conservative root functional strategy, also positively affects $R_a/R_s$. These seemingly contrasting results provide evidence for the multidimensionality of root trait-physiological relationships, where orthogonal root functional traits from alternative root functional (*i.e.*, acquisitive vs. conservative) strategies can have similar effects on a physiological response or ecosystem process (Bardgett et al., 2014; Bergmann et al., 2020; Freschet et al., 2020; Laliberté, 2017; Weemstra et al., 2016).

Physical models of $R_s$ within the soil seldom include root properties (Blagodatsky and Smith, 2012; Reichstein and Beer, 2008). However, a compelling case for including aggregate (*i.e.*, community level) root system traits within the root-dense upper soil can be made. The physical (*i.e.*, length and density), chemical (*e.g.*, tissue properties and exudates), and physiological root traits (*e.g.*, mycorrhizal affinities) modulate the physical soil environment through their feedbacks on the flow of water, gasses, and solutes through the root-soil system. For example, using state-of-the-art rhizotron technology in a mixed temperate forest, total daily $R_s$ was found to be correlated with variation in total fine root length, which was not related to short-term changes in soil volumetric water content (Vargas and Allen, 2008). Thus, the physical presence of roots and variation in their morphological traits affect $R_s$ magnitude.

Root traits are also related to the biological components of the root-soil system. A recent study showed that the ratio of root-inhabiting fungi to bacteria decreased with increasing SRL, and that microbial community composition (*i.e.*, the ratio of gram-positive to gram-negative bacteria) was related to RTD (Wan et al., 2021). Such effects of root functional traits on soil microbial communities and hence soil functioning likely superseded effects of leaf litter or individual tree effects, illustrating the need to incorporate root functional traits into our understanding and modeling of soil biogeochemical dynamics. Consistent with the findings of this research, a second recent study demonstrated how $R_s$ increased with SRL, $N_{root,}$ and with increasing $R_r$ through effects on $R_a$ in riparian agrosystems (Borden et al., 2021). Borden et al. (2021) demonstrated how root traits can alter microbial abundance and composition of the rhizosphere to impact $R_h$, showing clear positive effects of root diameter and root C:N on $R_s$, which we found some evidence for in our study of the native tree species in the temperate deciduous forest of Oak Ridge, Tennessee. A third recent study showed that the finest (*i.e.*, 1st and 2nd order) roots environmentally filter bacterial community composition of root tissues to the most significant degree relative to the soil bacterial communities and that microbial loads are largest on the most physiologically active fine roots (King et al., 2021). Linking such biological variation in microbial associations of tree roots at the root system (or even root order) level and evaluating their effects on soil biogeochemical processes via root physiology and functional traits holds excellent promise in deepening our understanding of root-level controls on $R_a$ and $R_h$ and their contributions to $R_s$.

## 5. Conclusion

Repeated measurements of $R_s$ for entire root systems and their surrounding soil *in situ* and some applied assumptions enabled our estimate that the contribution of $R_a$ to $R_s$ for functional entire root systems of 3 to 4 root orders ranges from 0 to 10 %, averaging 2–3%. Per unit mass, we estimate that $R_a$ was roughly 20 times greater than $R_h$. The $R_a/R_s$ fraction increased with greater SRL and root tip abundance, two traits characteristic of root system acquisitiveness, but also increased with greater RTD, which usually characterizes more-conservative root strategies. Specific respiration rates of excised root systems showed similar patterns concerning root functional strategy, being most strongly related to variation in $N_{root}$, which was arranged roughly opposite RTD in the root functional trait space and being more-weakly related to a tradeoff in root diameter vs. root tip abundance. Such variation in $R_r$ with root functional strategy translated to the variation in $R_a/R_s$, although not perfectly, pointing to interactions between $R_a$ and $R_h$ (*i.e.*, roots and soil microbes) which contribute to $R_s$. No clear patterns $R_a/R_s$ were found concerning mycorrhizal affinity of the 8 studied tree species, but this may be due to species selection and limited sample size.

Temporal and environmental variability were also essential modulators of $R_a/R_s$. The ratio peaked at the beginning of fall, which coincided with forest canopy leaf senescence, likely as allocation of labile C to roots increased. Higher soil moisture negatively affected the ratio, likely becuase soil wetting decreases $R_a$, potentially shifting metabolic activity from C allocation and transfer to water uptake or because of great $CO_2$ dissolution into soil-bound water. Warmer soil temperatures increased the ratio, probably through temperature effects on the enzymatic kinetics of root physiological processes and via increases in soil metabolic processes. Thus, individual root systems are physiologically dynamic within the soil microbiome, especially at the rhizosphere, however extending into the larger soil environment; the respiratory signal of functional root systems on $R_s$ is subtle yet evident.

## 6. Data availability

The dataset for the work has been archived Oak Ridge National Laboratory Terrestrial Ecosystem Science Focus area (ORNL TESSFA). It will be archived on the TESSFA data portal https://tes-sfa.ornl.gov/node/80, concurrently with publication.

Hogan JA, Labbé JL, Carell AA, Franklin J, Hoyt KP, Valverde-Barrantes OJ, Baraloto C & Warren JM. 2022. Belowground Respiration of a temperate deciduous forest – separating autotrophic vs. heterotrophic respiration from *in-situ* root respiration trays.

Oak Ridge National Laboratory, TES SFA, U.S. Department of Energy, Oak Ridge, Tennessee, U.S.A. https://doi.org/10.25581/ornlsfa.025/1838660.

Sequencing data for soil bacteria and fungi have been archived in a

sequence read archive (SRA) on GenBank – BioProject SRA # PRJNA786934: http://www.ncbi.nlm.nih.gov/bioproject/PRJNA786934.

## CRediT authorship contribution statement

**J. Aaron Hogan:** Conceptualization, Methodology, Validation, Investigation, Formal analysis, Data curation, Writing – original draft, Funding acquisition. **Jessy L. Labbé:** Writing – review & editing, Supervision, Project administration. **Alyssa A. Carrell:** Investigation, Formal analysis, Data curation, Writing – review & editing. **Jennifer Franklin:** Investigation, Supervision, Writing – review & editing. **Kevin P. Hoyt:** Conceptualization, Project administration, Resources. **Oscar J. Valverde-Barrantes:** Conceptualization, Writing – review & editing. **Christopher Baraloto:** Conceptualization, Writing – review & editing, Supervision. **Jeffrey M. Warren:** Conceptualization, Resources, Writing – review & editing, Supervision, Project administration, Funding acquisition.

## Declaration of Competing Interest

This manuscript has been authored by UT-Battelle, LLC under Contract No. DE-AC05-00OR22725 with the US Department of Energy. The United States Government retains and the publisher, by accepting the article for publication, acknowledges that the United States Government retains a non-exclusive, paid-up, irrevocable, worldwide license to publish or reproduce the published form of this manuscript, or allow others to do so, for United States Government purposes. The Department of Energy will provide public access to these results of federally sponsored research in accordance with the DOE Public Access Plan (http://energy.gov/downloads/doe-public-access-plan).

## Data availability

The data are archived at the shared link (see manuscript)

## Acknowledgments

This work was completed in collaboration with the Forest Resources AgResearch and Education Center at the University of Tennessee. We thank Mindy Clark, Zach Ziegler, Jacob Wyre, Joe Gebhart and Yvonne Hitchcock for their help in the field. We are very grateful to Jana Philips, Joanne Childs, and Deanne Brice at the Division of Environmental Science at Oak Ridge National Laboratory for their help with the soil chloroform extractions and leaf nutrient analyses. We thank Sara Wilson at the Blue Carbon Lab at Florida International University for help with root tissue nutrient analyses. We also thank Cici Hall from Li-COR Inc. for her help with troubleshooting many questions and providing expertise on gas exchange measurements. Research sponsored by the U. S. Department of Energy (DOE), by the DOE Office of Science, Office of Biological and Environmental Research, and by Office of Science, Office of Workforce Development for Teachers and Scientists, Office of Science Graduate Student Research (SCGSR) program. The SCGSR program is administered by the Oak Ridge Institute for Science and Education (ORISE) for the DOE. ORISE is managed by ORAU under contract number DE-AC05-06OR23100. Oak Ridge National Laboratory (ORNL) is managed by UT-Battelle, LLC, for the DOE under contract DE-AC05-00OR22725.

## Appendix A. Supplementary data

Supplementary data to this article can be found online at https://doi.org/10.1016/j.geoderma.2023.116414.

## References

Abramoff, R.Z., Finzi, A.C., 2016. Seasonality and partitioning of root allocation to rhizosphere soils in a midlatitude forest. Ecosphere 7 (11), e01547.
Adler, P.B., Salguero-Gómez, R., Compagnoni, A., Hsu, J.S., Ray-Mukherjee, J., Mbeau-Ache, C., Franco, M., 2014. Functional traits explain variation in plant life history strategies. Proc. Natl. Acad. Sci. USA 111 (2), 740–745.
Atkin, O.K., Edwards, E.J., Loveys, B.R., 2000. Response of root respiration to changes in temperature and its relevance to global warming. New Phytologist 147 (1), 141–154.
Bardgett, R.D., Mommer, L., De Vries, F.T., 2014. Going underground: root traits as drivers of ecosystem processes. Trends Ecol. Evol. 29 (12), 692–699.
Bates, D., Mächler, M., Bolker, B., Walker, S., 2015. Fitting Linear mixed-effects models using lme4. J. Stat. Softw. 67 (1), 1–48.
Bennett, J.A., Maherali, H., Reinhart, K.O., Lekberg, Y., Hart, M.M., Klironomos, J., 2017. Plant-soil feedbacks and mycorrhizal type influence temperate forest population dynamics. Science 355 (6321), 181–184.
Bergmann, J., Weigelt, A., van der Plas, F., Laughlin, D.C., Kuyper, T.W., Guerrero-Ramirez, N., Valverde-Barrantes, O.J., Bruelheide, H., Freschet, G.T., Iversen, C.M., Kattge, J., McCormack, M.L., Meier, I.C., Rillig, M.C., Roumet, C., Semchenko, M., Sweeney, C.J., van Ruijven, J., York, L.M., Mommer, L., 2020. The fungal collaboration gradient dominates the root economics space in plants. Sci. Adv. 6 (27), eaba3756.
Blagodatsky, S., Smith, P., 2012. Soil physics meets soil biology: towards better mechanistic prediction of greenhouse gas emissions from soil. Soil Biol. Biochem. 47, 78–92.
Bolyen, E., Rideout, J.R., Dillon, M.R., Bokulich, N.A., Abnet, C.C., Al-Ghalith, G.A., Alexander, H., Alm, E.J., Arumugam, M., Asnicar, F., 2019. Reproducible, interactive, scalable and extensible microbiome data science using QIIME 2. Nat. Biotechnol. 37 (8), 852–857.
Bond-Lamberty, B., Wang, C., Gower, S.T., 2004. A global relationship between the heterotrophic and autotrophic components of soil respiration? Glob. Change Biol. 10 (10), 1756–1766.
Bond-Lamberty, B., Bronson, D., Bladyka, E., Gower, S.T., 2011. A comparison of trenched plot techniques for partitioning soil respiration. Soil Biol. Biochem. 43 (10), 2108–2114.
Bond-Lamberty, B., Thomson, A., 2010a. A global database of soil respiration data. Biogeosciences 7 (6), 1915–1926.
Bond-Lamberty, B., Thomson, A., 2010b. Temperature-associated increases in the global soil respiration record. Nature 464 (7288), 579–582.
Borden, K.A., Mafa-Attoye, T.G., Dunfield, K.E., Thevathasan, N.V., Gordon, A.M., Isaac, M.E., 2021. Root functional trait and soil microbial coordination: implications for soil respiration in riparian agroecosystems. Front. Plant Sci. 12, 681113.
Bouma, T.J., Nielsen, K.L., Eissenstat, D.M., Lynch, J.P., 1997. Estimating respiration of roots in soil: Interactions with soil $CO_2$, soil temperature and soil water content. Plant Soil 195 (2), 221–232.
Brookes, P., Landman, A., Pruden, G., Jenkinson, D., 1985. Chloroform fumigation and the release of soil nitrogen: a rapid direct extraction method to measure microbial biomass nitrogen in soil. Soil Biol. Biochem. 17 (6), 837–842.
Bryla, D.R., Eissenstat, D.M., 2005. Respiratory Costs of Mycorrhizal Associations. In: Lambers, H., Ribas-Carbo, M. (Eds.), Advances in Photosynthesis and RespirationPlant Respiration. Springer-Verlag, Berlin/Heidelberg, pp. 207–224.
Burton, A., Pregitzer, K., Ruess, R., Hendrick, R., Allen, M., 2002. Root respiration in North American forests: effects of nitrogen concentration and temperature across biomes. Oecologia 131 (4), 559–568.
Burton, A.J., Pregitzer, K.S., 2003. Field measurements of root respiration indicate little to no seasonal temperature acclimation for sugar maple and red pine. Tree Physiol. 23 (4), 273–280.
Campbell, J.L., Law, B.E., 2005. Forest soil respiration across three climatically distinct chronosequences in Oregon. Biogeochemistry 73 (1), 109–125.
Ceccon, C., Tagliavini, M., Schmitt, A.O., Eissenstat, D.M., Epron, D., 2016. Untangling the effects of root age and tissue nitrogen on root respiration in Populus tremuloides at different nitrogen supply. Tree Physiol. 36 (5), 618–627.
Chen, G.-S., Yang, Y.-S., Guo, J.-F., Xie, J.-S., Yang, Z.-J., 2011. Relationships between carbon allocation and partitioning of soil respiration across world mature forests. Plant Ecol. 212 (2), 195–206.
Chen, G., Yang, Y., Robinson, D., 2014. Allometric constraints on, and tradeoffs in, belowground carbon allocation and their control of soil respiration across global forest ecosystems. Glob. Change Biol. 20 (5), 1674–1684.
Cleveland, C., Nemergut, D., Schmidt, S., Townsend, A., 2007. Increases in soil respiration following labile carbon additions linked to rapid shifts in soil microbial community composition. Biogeochemistry 82 (3), 229–240.
Comas, L., Bouma, T., Eissenstat, D., 2002. Linking root traits to potential growth rate in six temperate tree species. Oecologia 132 (1), 34–43.
Comas, L.H., Callahan, H.S., Midford, P.E., 2014. Patterns in root traits of woody species hosting arbuscular and ectomycorrhizas: implications for the evolution of belowground strategies. Ecol. and Evol. 4 (15), 2979–2990.
Condron, L., Stark, C., O'Callaghan, M., Clinton, P., Huang, Z., 2010. The role of microbial communities in the formation and decomposition of soil organic matter, Soil microbiology and sustainable crop production. In: Dixon, G.R., Tilston, E.L. (Eds.), Soil Microbiology and Sustainable Crop Production. Springer Netherlands, Dordrecht, pp. 81–118.
Craine, J.M., Dybzinski, R., 2013. Mechanisms of plant competition for nutrients, water and light. Funct. Ecol. 27 (4), 833–840.
Davidson, E.A., Janssens, I.A., 2006. Temperature sensitivity of soil carbon decomposition and feedbacks to climate change. Nature 440 (7081), 165–173.

Delcourt, H., Delcourt, P., 2000. Eastern Deciduous Forests of Eastern North America. In: Barbour, M., Billings, W. (Eds.), North American terrestrial vegetation. Cambridge University Press, Cambridge, UK, pp. 357–395.
Díaz, S., Kattge, J., Cornelissen, J.H.C., Wright, I.J., Lavorel, S., Dray, S., Reu, B., Kleyer, M., Wirth, C., Colin Prentice, I., Garnier, E., Bönisch, G., Westoby, M., Poorter, H., Reich, P.B., Moles, A.T., Dickie, J., Gillison, A.N., Zanne, A.E., Chave, J., Joseph Wright, S., Sheremet'ev, S.N., Jactel, H., Baraloto, C., Cerabolini, B., Pierce, S., Shipley, B., Kirkup, D., Casanoves, F., Joswig, J.S., Günther, A., Falczuk, V., Rüger, N., Mahecha, M.D., Gorné, L.D., 2016. The global spectrum of plant form and function. Nature 529 (7585), 167–171.
Edwards, N.T., Sollins, P., 1973. Continuous measurement of carbon dioxide evolution from partitioned forest floor components. Ecology 54 (2), 406–412.
Eissenstat, D.M., Kucharski, J.M., Zadworny, M., Adams, T.S., Koide, R.T., 2015. Linking root traits to nutrient foraging in arbuscular mycorrhizal trees in a temperate forest. New Phytol. 208 (1), 114–124.
Epron, D., Farque, L., Lucot, E., Badot, P.-M., 1999. Soil $CO_2$ efflux in a beech forest: the contribution of root respiration. Ann. For. Sci. 56 (4), 289–295.
Estaki, M., Jiang, L., Bokulich, N., McDonald, D., González, A., Kosciolek, T., Martino, C., Zhu, Q., Birmingham, A., Vázquez-Baeza, Y., Dillon, M., Bolyen, E., Caporaso, J., Knight, R., 2020. QIIME 2 enables comprehensive end-to-end analysis of diverse microbiome data and comparative studies with publicly available data. Curr. Protocols Bioinformatics 70 (1), e100.
Fang, C., Moncrieff, J.B., 1999. A model for soil $CO_2$ production and transport 1: model development. Agric. For. Meteorol. 95 (4), 225–236.
Freschet, G.T., Roumet, C., Comas, L.H., Weemstra, M., Bengough, A.G., Rewald, B., Bardgett, R.D., De Deyn, G.B., Johnson, D., Klimešová, J., Lukac, M., McCormack, M. L., Meier, I.C., Pagès, L., Poorter, H., Prieto, I., Wurzburger, N., Zadworny, M., Bagniewska-Zadworna, A., Blancaflor, E.B., Brunner, I., Gessler, A., Hobbie, S.E., Iversen, C.M., Mommer, L., Picon-Cochard, C., Postma, J.A., Rose, L., Ryser, P., Scherer-Lorenzen, M., Soudzilovskaia, N.A., Sun, T., Valverde-Barrantes, O.J., Weigelt, A., York, L.M., Stokes, A., 2020. Root traits as drivers of plant and ecosystem functioning: current understanding, pitfalls and future research needs. New Phytologist 232 (3), 1123–1158.
Gao, J., Zhou, M., Shao, J., Zhou, G., Liu, R., Zhou, L., Liu, H., He, Y., Chen, Y., Zhou, X., 2021. Fine root trait-function relationships affected by mycorrhizal type and climate. Geoderma 394, 115011.
Hanson, P.J., Edwards, N.T., Garten, C.T., Andrews, J.A., 2000. Separating root and soil microbial contributions to soil respiration: a review of methods and observations. Biogeochemistry 48 (1), 115–146.
Hill, P.W., Garnett, M.H., Farrar, J., Iqbal, Z., Khalid, M., Soleman, N., Jones, D.L., 2015. Living roots magnify the response of soil organic carbon decomposition to temperature in temperate grassland. Glob. Change Biol. 21 (3), 1368–1375.
Högberg, P., Nordgren, A., Buchmann, N., Taylor, A.F.S., Ekblad, A., Högberg, M.N., Nyberg, G., Ottosson-Löfvenius, M., Read, D.J., 2001. Large-scale forest girdling shows that current photosynthesis drives soil respiration. Nature 411 (6839), 789–792.
Insam, H., 2001. Developments in soil microbiology since the mid-1960s. Geoderma 100 (3–4), 389–402.
Janssens, I.A., Lankreijer, H., Matteucci, G., Kowalski, A.S., Buchmann, N., Epron, D., Pilegaard, K., Kutsch, W., Longdoz, B., Grünwald, T., Montagnani, L., Dore, S., Rebmann, C., Moors, E.J., Grelle, A., Rannik, Ü., Morgenstern, K., Oltchev, S., Clement, R., Guðmundsson, J., Minerbi, S., Berbigier, P., Ibrom, A., Moncrieff, J., Aubinet, M., Bernhofer, C., Jensen, N.O., Vesala, T., Granier, A., Schulze, E.-D., Lindroth, A., Dolman, A.J., Jarvis, P.G., Ceulemans, R., Valentini, R., 2001. Productivity overshadows temperature in determining soil and ecosystem respiration across European forests. Glob. Change Biol. 7 (3), 269–278.
Jia, S., McLaughlin, N.B., Gu, J., Li, X., Wang, Z., 2013. Relationships between root respiration rate and root morphology, chemistry and anatomy in Larix gmelinii and Fraxinus mandshurica. Tree Physiol. 33 (6), 579–589.
Jian, J., Frissell, M., Hao, D., Tang, X., Berryman, E., Bond-Lamberty, B., 2022. The global contribution of roots to total soil respiration. Global Ecol. and Biogeogr. 31 (4), 685–699.
Johnson, D.J., Clay, K., Phillips, R.P., 2018. Mycorrhizal associations and the spatial structure of an old-growth forest community. Oecologia 186 (1), 195–204.
Katabuchi, M., 2015. LeafArea: an R package for rapid digital image analysis of leaf area. Ecol. Res. 30 (6), 1073–1077.
Keller, A.B., Brzostek, E.B., Craig, M.E., Fisher, J.B., Phillips, R.P., 2021. Root -derived inputs are major contributors to soil carbon in temperate forests, but vary by mycorrhizal type. Ecol. Lett. 24 (4), 626–635.
King, W.L., Yates, C.F., Guo, J., Fleishman, S.M., Trexler, R.V., Centinari, M., Bell, T.H., Eissenstat, D.M., 2021. The hierarchy of root branching order determines bacterial composition, microbial carrying capacity and microbial filtering. Commun. Biol. 4 (1), 1–9.
Kuznetsova, A., Brockhoff, P.B., Christensen, R.H.B., 2017. lmerTest package: tests in linear mixed effects models. J. Stat. Softw. 82 (13), 26.
Kuzyakov, Y., 2006. Sources of $CO_2$ efflux from soil and review of partitioning methods. Soil Biol. Biochem. 38 (3), 425–448.
Laliberté, E., 2017. Below-ground frontiers in trait-based plant ecology. New Phytologist 213 (4), 1597–1603.
Lang, A.K., Jevon, F.V., Ayres, M.P., Matthes, J.H., 2020. Higher soil respiration rate beneath arbuscular mycorrhizal trees in a northern hardwood forest is driven by associated soil properties. Ecosystems 23 (6), 1243–1253.
Lavigne, M.B., Roster, R.J., Goodine, G., Bernier, P.Y., Robitaille, G., 2003. Soil respiration responses are controlled more by roots than by decomposition in balsam fir ecosystems. Can. J. For. Res. 33 (9), 1744–1753.
Liming, Y., Dijkstra, F.E., Phillips, R.E., Zhu, B., Wang, P., Chen, W., 2021. Arbuscular mycorrhizal trees cause a higher carbon to nitrogen ratio of soil organic matter decomposition via rhizosphere priming than ectomycorrhizal trees. Soil Biol. Biochem. 157, 108246.
Lüdecke, D., 2018. sjPlot: Data visualization for statistics in social science. R package version 2(1).
Luxmoore, R.J., 1982. Physical characteristics of soils of the southern region: Fullerton and Sequoia series. ORNL-5868, Oak Ridge National Lab., TN (USA).
Madani, N., Parazoo, N.C., Kimball, J.S., Ballantyne, A.P., Reichle, R.H., Maneta, M., Saatchi, S., Palmer, P., Liu, Z., Tagesson, T., 2020. Recent amplified global gross primary productivity due to temperature increase is offset by reducted productivity due to water contsrtians. AGU Adv. 1 e2020AV000180.
Makita, N., Kosugi, Y., Dannoura, M., Takanashi, S., Niiyama, K., Kassim, A.R., Nik, A.R., 2012. Patterns of root respiration rates and morphological traits in 13 tree species in a tropical forest. Tree Physiol. 32 (3), 303–312.
Makita, N., Hirano, Y., Sugimoto, T., Tanikawa, T., Ishii, H., 2015. Intraspecific variation in fine root respiration and morphology in response to *in situ* soil nitrogen fertility in a 100-year-old *Chamaecyparis obtusa* forest. Oecologia 179 (4), 959–967.
McCormack, M.L., Adams, T.S., Smithwick, E.A.H., Eissenstat, D.M., 2012. Predicting fine root lifespan from plant functional traits in temperate trees. New Phytologist 195 (4), 823–831.
McCormack, M.L., Dickie, I.A., Eissenstat, D.M., Fahey, T.J., Fernandez, C.W., Guo, D., Helmisaari, H.S., Hobbie, E.A., Iversen, C.M., Jackson, R.B., 2015. Redefining fine roots improves understanding of below-ground contributions to terrestrial biosphere processes. New Phytologist 207 (3), 505–518.
McCormack, M.L., Iversen, C.M., 2019. Physical and functional constraints on viable belowground acquisition strategies. Front. Plant Sci. 10 (1215).
McMurdie, P.J., Holmes, S., 2013. phyloseq: an R package for reproducible interactive analysis and graphics of microbiome census data. PLoS One 8 (4), e61217.
Menne, M.J., Durre, I., Vose, R.S., Gleason, B.E., Houston, T.G., 2012. An overview of the global historical climatology network-daily database. J. Atmos. Oceanic Technol. 29 (7), 897–910 dataset accessed on 11/2/2020.
Metcalfe, D.B., Fisher, R., Wardle, D.A., 2011. Plant communities as drivers of soil respiration: pathways, mechanisms, and significance for global change. Biogeosciences 8 (8), 2047–2061.
Nilsson, R.H., Larsson, K.-H., Taylor, A.F.S., Bengtsson-Palme, J., Jeppesen, T.S., Schigel, D., Kennedy, P., Picard, K., Glöckner, F.O., Tedersoo, L., Saar, I., Kõljalg, U., Abarenkov, K., 2018. The UNITE database for molecular identification of fungi: handling dark taxa and parallel taxonomic classifications. Nucleic Acids Res. 47 (D1), D259–D264.
Noh, N.J., Crous, K.Y., Li, J., Choury, Z., Barton, C.V., Arndt, S.K., Reich, P.B., Tjoelker, M.G., Pendall, E., 2020. Does root respiration in Australian rainforest tree seedlings acclimate to experimental warming? Tree Physiol. 40 (9), 1192–1204.
Palta, J.A., Nobel, P.S., 1989. Root respiration for *Agave deserti*: influence of temperature, water status and root age on daily patterns. J. Exp. Bot. 40 (2), 181–186.
Paradiso, E., Jevon, F., Matthes, J., 2019. Fine root respiration is more strongly correlated with root traits than tree species identity. Ecosphere 10, e02944.
Pausch, J., Kuzyakov, Y., 2018. Carbon input by roots into the soil: quantification of rhizodeposition from root to ecosystem scale. Glob. Change Biol. 24 (1), 1–12.
Pregitzer, K.S., Burton, A.J., King, J.S., Zak, D.R., 2008. Soil respiration, root biomass, and root turnover following long-term exposure of northern forests to elevated atmospheric $CO_2$ and tropospheric $O_3$. New Phytologist 180 (1), 153–161.
Pruesse, E., Peplies, J., Glöckner, F.O., 2012. SINA: accurate high-throughput multiple sequence alignment of ribosomal RNA genes. Bioinformatics 28 (14), 1823–1829.
R Core Team, 2020. R: A language and environment for statistical computing (4.0. 3) [Computer software]. R Foundation for Statistical Computing. Retrieved from http://www.R-project.org.
Raich, J.W., Nadelhoffer, K.J., 1989. Belowground carbon allocation in forest ecosystems: global trends. Ecology 70 (5), 1346–1354.
Raich, J.W., Potter, C.S., Bhagawati, D., 2002. Interannual variability in global soil respiration, 1980–94. Glob. Change Biol. 8 (8), 800–812.
Raich, J.W., Tufekciogul, A., 2000. Vegetation and soil respiration: correlations and controls. Biogeochemistry 48 (1), 71–90.
Reich, P.B., 2014. The world-wide 'fast–slow' plant economics spectrum: a traits manifesto. J. Ecol. 102 (2), 275–301.
Reich, P.B., Tjoelker, M.G., Pregitzer, K.S., Wright, I.J., Oleksyn, J., Machado, J.L., 2008. Scaling of respiration to nitrogen in leaves, stems and roots of higher land plants. Ecol. Lett. 11 (8), 793–801.
Reichstein, M., Beer, C., 2008. Soil respiration across scales: the importance of a model–data integration framework for data interpretation. J. Plant Nutr. Soil Sci. 171 (3), 344–354.
Rossi, L.M., Mao, Z., Merino-Martin, L., Roumet, C., Fort, F., Taugourdeau, O., Boukcim, H., Fourtier, S., Del Rey-Granado, M., Chevallier, T., 2020. Pathways to persistence: plant root traits alter carbon accumulation in different soil carbon pools. Plant Soil 452 (1), 457–478.
Roumet, C., Birouste, M., Picon-Cochard, C., Ghestem, M., Normaniza, O., Vigron-Brenas, S., Cao, K., Stokes, A., 2016. Root structure-function relationships in 74 species: evidence of a root economics spectrum related to carbon economy. New Phytologist 210 (3), 815–826.
Ryan, M.G., Law, B.E., 2005. Interpreting, measuring, and modeling soil respiration. Biogeochemistry 73 (1), 3–27.
Soudzilovskaia, N.A., van Bodegom, P.M., Terrer, C., Zelfde, M.V.T., McCallum, I., Luke McCormack, M., Fisher, J.B., Brundrett, M.C., de Sá, N.C., Tedersoo, L., 2019. Global mycorrhizal plant distribution linked to terrestrial carbon stocks. Nat. Commun. 10 (1), 5077.

Taylor, M.K., Lankau, R.A., Wurzburger, N., 2016. Mycorrhizal associations of trees have different indirect effects on organic matter decomposition. J. Ecol. 104 (6), 1576–1584.
Teodosio, B., Pauwels, V.R.N., Loheide II, S.P., Daly, E., 2017. Relationship between root water uptake and soil respiration: a modeling perspective. J. Geophys. Res.: Biogeosci. 122 (8), 1954–1968.
Trevors, J., 1996. Sterilization and inhibition of microbial activity in soil. J. Microbiol. Methods 26 (1–2), 53–59.
Trumbore, S., 2006. Carbon respired by terrestrial ecosystems–recent progress and challenges. Glob. Change Biol. 12 (2), 141–153.
Valverde-Barrantes, O.J., Freschet, G.T., Roumet, C., Blackwood, C.B., 2017. A worldview of root traits: the influence of ancestry, growth form, climate and mycorrhizal association on the functional trait variation of fine-root tissues in seed plants. New Phytologist 215 (4), 1562–1573.
Vargas, R., Allen, M.F., 2008. Dynamics of fine root, fungal rhizomorphs, and soil respiration in a mixed temperate forest: integrating sensors and observations. Vadose Zone J. 7 (3), 1055–1064.
Wan, X., Chen, X., Huang, Z., 2021. Contribution of root traits to variations in soil microbial biomass and community composition. Plant Soil 460, 482–495.
Wang, C., Yang, J., Zhang, Q., 2006. Soil respiration in six temperate forests in China. Glob. Change Biol. 12 (11), 2103–2114.
Wang, C., Ma, Y., Trogisch, S., Huang, Y., Geng, Y., Scherer-Lorenzen, M., He, J.-S., 2017. Soil respiration is driven by fine root biomass along a forest chronosequence in subtropical China. J. Plant Ecol. 10 (1), 36–46.
Warren, J.M., Iversen, C.M., Garten Jr, C.T., Norby, R.J., Childs, J., Brice, D., Evans, R. M., Gu, L., Thornton, P., Weston, D.J., 2011. Timing and magnitude of C partitioning through a young loblolly pine (*Pinus taeda* L.) stand using $^{13}C$ labeling and shade treatments. Tree Physiol. 32 (6), 799–813.
Warren, J.M., Hanson, P.J., Iversen, C.M., Kumar, J., Walker, A.P., Wullschleger, S.D., 2015. Root structural and functional dynamics in terrestrial biosphere models – evaluation and recommendations. New Phytologist 205 (1), 59–78.
Weemstra, M., Mommer, L., Visser, E.J., Ruijven, J., Kuyper, T.W., Mohren, G.M., Sterck, F.J., 2016. Towards a multidimensional root trait framework: a tree root review. New Phytologist 211 (4), 1159–1169.
Weigelt, A., Mommer, L., Andraczek, K., Iversen, C.M., Bergmann, J., Bruelheide, H., Fan, Y., Freschet, G.T., Guerrero-Ramírez, N.R., Kattge, J., Kuyper, T.W., Laughlin, D.C., Meier, I.C., van der Plas, F., Poorter, H., Roumet, C., van Ruijven, J., Sabatini, F.M., Semchenko, M., Sweeney, C.J., Valverde-Barrantes, O.J., York, L.M., McCormack, M.L., 2021. An integrated framework of plant form and function: the belowground perspective. New Phytologist 232 (1), 42–59.
Wurzburger, N., Brookshire, E.N.J., 2017. Experimental evidence that mycorrhizal nitrogen strategies affect soil carbon. Ecology 98 (6), 1491–1497.
Xu, M., Shang, H., 2016. Contribution of soil respiration to the global carbon equation. J. Plant Physiol. 203, 16–28.
Yan, H., Freschet, G.T., Wang, H., Hogan, J.A., Li, S., Valverde-Barrantes, O.J., Fu, X., Wang, R., Dai, X., Jiang, L., Meng, S., Yang, F., Zhang, M., Kou, L., 2022. Mycorrhizal symbiosis pathway and edaphic fertility frame root economics space among tree species. New Phytologist 234 (5), 1639–1653.
Yang, J., Wang, C., 2006. Partitioning soil respiration of temperate forest ecosystems in northeastern China. Acta Ecologica Sinica 26 (6), 1640–1646.